

A Combination of Preliminary Electroweak Measurements and Constraints on the Standard Model

The LEP Collaborations* ALEPH, DELPHI, L3, OPAL, the LEP
Electroweak Working Group[†]
and the SLD Heavy Flavour Group[‡].
Prepared from Contributions
to the 28th International Conference on High Energy Physics, Warsaw, Poland,
25-31 July 1996.

Abstract

This note presents a combination of published and preliminary electroweak results from the four LEP collaborations and the SLD collaboration which were prepared for the 1996 summer conferences. Averages of the results concerning electroweak physics are presented. They are derived from the measurements of hadronic and leptonic cross sections, the leptonic forward-backward asymmetries, the τ polarisation asymmetries, the $b\bar{b}$ and $c\bar{c}$ partial widths and forward-backward asymmetries and the $q\bar{q}$ charge asymmetry. Almost every measurement including the LEP beam energy calibration has been updated with respect to the summer 1995 conferences. The results are compared to precise electroweak measurements from other experiments. The parameters of the Standard Model are evaluated, first using the combined LEP electroweak measurements, and then using the full set of precise electroweak results.

*The LEP Collaborations each take responsibility for the preliminary data of their own experiment.

[†]The present members of the LEP Electroweak Working Group are: D. Abbaneo, J. Alcaraz, P. Antilogus, T. Behnke, B. Bertucci, D. Bloch, A. Blondel, D.G. Charlton, R. Clare, P. Clarke, S. Dutta, M. Elsing, S. Ganguli, M.W. Grunewald, A. Gurtu, K. Hamacher, C.M. Hawkes, M. Hildreth, R.W.L. Jones, W. Lohmann, T. Kawamoto, Y. Khokhlov, C. Mariotti, M. Martinez, K. Mönig, M. Morii, A. Nippe, A. Olshevsky, Ch. Paus, M. Pepe-Altarelli, B. Pietrzyk, G. Quast, P. Renton, D. Reid, M. Roney, D. Schlatter, R. Sobie, R. Tenchini, F. Teubert, I. Tomalin, and P.S. Wells.

[‡]The representatives from SLD are: B. Schumm and D. Su.

1 Introduction

The four LEP experiments have previously presented [1] parameters derived from the Z resonance using published and preliminary results based on data recorded until the end of 1994. These results represented the status of the analyses in summer 1995.

Since then several additional preliminary results have become available, including results from the 1995 Z energy scan. To allow a quick assessment, a box highlighting the updates is given at the beginning of each section. Results from data taken at energies significantly above the Z pole are not included in the note. Results from the high energy (130–140 GeV) run at the end of 1995 are presented elsewhere [2].

The LEP data consist of the hadronic and leptonic cross sections, the leptonic forward-backward asymmetries, the τ polarisation asymmetries, the $b\bar{b}$ and $c\bar{c}$ partial widths and forward-backward asymmetries and the $q\bar{q}$ charge asymmetry. In addition, the measurement of the $b\bar{b}$ partial width and left-right-forward-backward asymmetries for b and c quarks from SLD are treated consistently with the LEP data. Many technical aspects of their combination have already been described in References 3, 4 and references therein. It should be stressed that several measurements included in the current combination are still preliminary.

This note is organised in the following manner:

Section 2 Z line shape and leptonic forward-backward asymmetries;

Section 3 τ polarisation;

Section 4 Heavy flavour analyses;

Section 5 Inclusive hadronic charge asymmetry;

Section 6 Interpretation of the results, including the combination of results from LEP, SLD, neutrino interaction experiments and W and top mass measurements from CDF and DØ;

Section 7 Prospects for the Future.

2 Z Lineshape and Lepton Forward-Backward Asymmetries

Updates from last year:

Preliminary results are available from analyses of the 1995 energy scan. The calibration of the LEP beam energy for the 1993 scan has been revised as a result of new information available in 1995. Several of the 1993/1994 preliminary analyses have been updated with reduced systematic errors, including reduced luminosity measurement errors. Also the theoretical error on the luminosity measurements has been reduced.

The 1995 energy scan resulted in each experiment collecting approximately 40 pb^{-1} of data, of which 18 pb^{-1} was recorded at two off-peak points with centre-of-mass energies, \sqrt{s} , 1.8 GeV above and below the Z peak. This almost doubles the data available for precision measurements of m_Z and Γ_Z . At the present time three of the experiments have preliminary analyses using both cross sections and lepton forward backward asymmetries; OPAL has only asymmetry results available for the present.

The results presented here are based on these new data combined with those recorded in previous years. This includes the data taken during the energy scans in 1990 and 1991 in the range $|\sqrt{s} - m_Z| < 3$ GeV, the data collected at the Z peak in 1992 and preliminary analyses of the energy scan in 1993 ($|\sqrt{s} - m_Z| < 1.8$ GeV) and the peak running in 1994. The total statistics and the systematic errors on the individual analyses of the four LEP collaborations are given in Tables 1 and 2. Details of the individual analyses can be found in References 5–8.

		ALEPH	DELPHI	L3	OPAL	LEP
$q\bar{q}$	'90-'91	451	357	416	454	1678
	'92	680	697	678	733	2788
	'93 prel.	640	677	646	646	2609
	'94 prel.	1654	1241	1307	1524	5726
	'95 prel.	739	584	311	–	1634
	total	4164	3556	3358	3357	14435
$\ell^+\ell^-$	'90-'91	55	36	40	58	189
	'92	82	70	58	88	298
	'93 prel.	78	74	64	82	298
	'94 prel.	190	129	127	184	630
	'95 prel.	80	67	28	42	217
	total	485	376	317	454	1632

Table 1: The LEP statistics in units of 10^3 events used for the analysis of the Z line shape and lepton forward-backward asymmetries. Not all experiments have used the full 1995 data set for the present results.

	ALEPH			DELPHI			L3			OPAL		
	'93 prel.	'94 prel.	'95 prel.	'93 prel.	'94 prel.	'95 prel.	'93 prel.	'94 prel.	'95 prel.	'93 prel.	'94 prel.	'95 prel.
$\mathcal{L}^{\text{exp. (b)}}$	0.087%	0.073%	0.097%	0.24%	0.09%	0.09%	0.10%	0.078%	0.128%	0.076%	0.079%	(^a)
σ_{had}	0.073%	0.073%	0.076%	0.10%	0.10%	0.10%	0.052%	0.051%	0.10%	0.15%	0.16%	(^a)
σ_e	0.50%	0.48%	0.47%	0.44%	0.50%	0.60%	0.30%	0.23%	1.0%	0.23%	0.24%	(^a)
σ_μ	0.25%	0.26%	0.25%	0.28%	0.30%	(^a)	0.31%	0.31%	1.0%	0.16%	0.15%	(^a)
σ_τ	0.34%	0.32%	0.39%	0.80%	0.60%	(^a)	0.67%	0.65%	0.60%	0.43%	0.46%	(^a)
A_{FB}^e	0.0031	0.0031	0.0028	0.0025	0.0022	0.0025	0.003	0.003	0.01	0.0016	0.0016	0.002
A_{FB}^μ	0.0005	0.0005	0.0005	0.0010	0.0015	0.0015	0.0008	0.0008	0.005	0.001	0.001	0.001
A_{FB}^τ	0.0009	0.0007	0.0009	0.0020	0.0020	0.0020	0.003	0.003	0.003	0.002	0.002	0.002

Table 2: The experimental systematic errors for the analysis of the Z line shape and lepton forward-backward asymmetries at the Z peak. The errors quoted do not include the common uncertainty due to the LEP energy calibration. The treatment of correlations between the errors for different years is described in References 5–8.

(^a)No preliminary result quoted yet.

(^b)In addition, there is a theoretical error for the calculation of the small angle Bhabha cross section of 0.11% [9], which has been treated as common to all experiments. For the present, the previous error of 0.16% [10] is used by ALEPH and DELPHI.

The measurement of the LEP beam energies, and the associated uncertainties, are important in the determination of the mass and width of the Z. In the previous note [1] the treatment of the LEP energies was that described in Reference 11. For the 1995 scan the instrumentation of LEP was improved by employing NMR devices in two LEP dipole magnets. Furthermore, in six fills resonant depolarisation measurements were made at both the beginning and end of fills and in two of these fills measurements were also made over a period of several hours. Preliminary results for the 1995 LEP

energies are available [12]. Using these new data, it has been found that there is a significant rise in energy during the course of a fill. Such a rise term was included in the previous analysis, but the magnitude of the rise observed in 1995 was considerably larger than that estimated for the 1993 scan. As a result the energy determinations for the 1993 scan and the 1994 peak data have been revised, although studies are still in progress and the results remain preliminary.

For the averaging of results the LEP experiments provide a standard set of 9 parameters describing the information contained in hadronic and leptonic cross sections and leptonic forward-backward asymmetries [3, 13]. These parameters have been corrected [14] for the effects of initial-state radiation as well as t -channel and s/t -interference in the case of e^+e^- final states. They are convenient for fitting and averaging since they have small correlations. The parameters are:

- The mass and total width of the Z boson, where the definition is based on the Breit-Wigner denominator ($s - m_Z^2 + is\Gamma_Z/m_Z$) [14].
- The hadronic pole cross section of Z exchange:

$$\sigma_h^0 \equiv \frac{12\pi}{m_Z^2} \frac{\Gamma_{ee}\Gamma_{\text{had}}}{\Gamma_Z^2}.$$

Here Γ_{ee} and Γ_{had} are the partial widths of the Z for decays into electrons and hadrons.

- The ratios:

$$R_e \equiv \Gamma_{\text{had}}/\Gamma_{ee}, \quad R_\mu \equiv \Gamma_{\text{had}}/\Gamma_{\mu\mu} \quad \text{and} \quad R_\tau \equiv \Gamma_{\text{had}}/\Gamma_{\tau\tau}. \quad (1)$$

Here $\Gamma_{\mu\mu}$ and $\Gamma_{\tau\tau}$ are the partial widths of the Z for the decays $Z \rightarrow \mu^+\mu^-$ and $Z \rightarrow \tau^+\tau^-$. Even under the assumption of lepton universality a small difference of 0.2% is expected between the values for R_e and R_μ , and the value for R_τ , owing to mass corrections to $\Gamma_{\tau\tau}$.

- The pole asymmetries, $A_{\text{FB}}^{0,e}$, $A_{\text{FB}}^{0,\mu}$ and $A_{\text{FB}}^{0,\tau}$, for the processes $e^+e^- \rightarrow e^+e^-$, $e^+e^- \rightarrow \mu^+\mu^-$ and $e^+e^- \rightarrow \tau^+\tau^-$. In terms of the effective vector and axial-vector neutral current couplings of fermions, g_{Vf} and g_{Af} , the pole asymmetries are expressed as:¹

$$A_{\text{FB}}^{0,f} \equiv \frac{3}{4} \mathcal{A}_e \mathcal{A}_f \quad (2)$$

with:

$$\mathcal{A}_f \equiv \frac{2g_{Vf}g_{Af}}{g_{Vf}^2 + g_{Af}^2}. \quad (3)$$

This set of 9 parameters does not describe the Z production and decay completely, because it does not include the interference of the Z exchange with the γ exchange. This contribution is investigated in a separate note [2]. For the results presented in this note, the γ -exchange contributions and the γZ interference terms are fixed to their Standard Model values.²

The four sets of 9 parameters provided by the LEP experiments are presented in Table 3. The covariance matrix of these parameters is constructed as described in Reference 13. It is constructed from the covariance matrices of the individual LEP experiments and common systematic errors. These common errors arise from the theoretical uncertainty in the luminosity normalisation affecting the

¹In the definition of $A_{\text{FB}}^{0,f}$, effects from γ exchange, γ/Z interference, as well as real and imaginary parts of the photon vacuum polarisation, are not included. They are accounted for explicitly in the fitting formulae used by the experiments, and are fixed to their Standard Model values.

²If instead the γZ interference terms are entirely determined from LEP cross-section data (including the 130-140 GeV data), the total error on the LEP average of m_Z increases from 2.0 MeV to 4.0 MeV [2].

hadronic pole cross section, $\Delta\sigma_h^0/\sigma_h^0 = 0.11\%$, from the uncertainty of the LEP centre-of-mass energy spread of about 1 MeV [15], resulting in $\Delta\Gamma_Z \approx 0.2$ MeV, and from the uncertainty in the LEP energy calibration. The latter uncertainty causes errors of $\Delta m_Z \approx 1.5$ MeV, $\Delta\Gamma_Z \approx 1.7$ MeV [12], and $\Delta A_{\text{FB}}^{0,\ell} \approx 0.0005$ for each lepton species ($\ell = e, \mu, \tau$). It should be noted that the error from the LEP beam energy spread has been reduced considerably from previous determinations. Full correlation between $A_{\text{FB}}^{0,\mu}$ and $A_{\text{FB}}^{0,\tau}$ and full anti-correlation between $A_{\text{FB}}^{0,e}$ and $A_{\text{FB}}^{0,\mu}$ or $A_{\text{FB}}^{0,\tau}$ is used. This anti-correlation for $A_{\text{FB}}^{0,e}$ is an approximation of the effect of the t -channel contribution for a typical LEP experimental acceptance for the e^+e^- final state. The combined parameter set and its correlation matrix are given in Tables 4 and 5.

	ALEPH	DELPHI	L3	OPAL
m_Z (GeV)	91.1873 ± 0.0030	91.1859 ± 0.0028	91.1883 ± 0.0029	91.1824 ± 0.0039
Γ_Z (GeV)	2.4950 ± 0.0047	2.4896 ± 0.0042	2.4996 ± 0.0043	2.4956 ± 0.0053
σ_h^0 (nb)	41.576 ± 0.083	41.566 ± 0.079	41.411 ± 0.074	41.53 ± 0.09
R_e	20.64 ± 0.09	20.93 ± 0.14	20.78 ± 0.11	20.82 ± 0.14
R_μ	20.88 ± 0.07	20.70 ± 0.09	20.84 ± 0.10	20.79 ± 0.07
R_τ	20.78 ± 0.08	20.78 ± 0.15	20.75 ± 0.14	20.99 ± 0.12
$A_{\text{FB}}^{0,e}$	0.0187 ± 0.0039	0.0179 ± 0.0051	0.0148 ± 0.0063	0.0104 ± 0.0052
$A_{\text{FB}}^{0,\mu}$	0.0179 ± 0.0025	0.0153 ± 0.0026	0.0176 ± 0.0035	0.0146 ± 0.0025
$A_{\text{FB}}^{0,\tau}$	0.0196 ± 0.0028	0.0223 ± 0.0039	0.0233 ± 0.0049	0.0178 ± 0.0034
$\chi^2/\text{d.o.f.}$	195/217	174/157	142/159	12/6 ^(a)

Table 3: Line shape and asymmetry parameters from 9-parameter fits to the data of the four LEP experiments.

^(a)This parameter set has been obtained from a parameter transformation applied to the 15 parameters of the OPAL fit [8], which treats the γZ interference terms for leptons as additional free parameters. The extra parameters for the γZ interference terms have been fixed to their Standard Model values in the transformation. The $\chi^2/\text{d.o.f.}$ for the 15-parameter fit to the data is 87/132.

Parameter	Average Value
m_Z (GeV)	91.1863 ± 0.0020
Γ_Z (GeV)	2.4946 ± 0.0027
σ_h^0 (nb)	41.508 ± 0.056
R_e	20.754 ± 0.057
R_μ	20.796 ± 0.040
R_τ	20.814 ± 0.055
$A_{\text{FB}}^{0,e}$	0.0160 ± 0.0024
$A_{\text{FB}}^{0,\mu}$	0.0162 ± 0.0013
$A_{\text{FB}}^{0,\tau}$	0.0201 ± 0.0018

Table 4: Average line shape and asymmetry parameters from the data of the four LEP experiments given in Table 3, without the assumption of lepton universality. The $\chi^2/\text{d.o.f.}$ of the average is 22/27.

The estimation of the common errors mentioned above which arise from the LEP energy calibration is more complicated than in previous years. This is partly due to the correlations in the LEP energy error matrix between the 1993 and 1995 scans and partly due to only three experiments having cross-section data available from the 1995 scan. The procedure adopted is the same approximate method as has been used for the previous note. Fits are performed to the data from a single experiment with all error components, other than those from the LEP energy, reduced so that they correspond

	m_Z	Γ_Z	σ_h^0	R_e	R_μ	R_τ	$A_{\text{FB}}^{0,e}$	$A_{\text{FB}}^{0,\mu}$	$A_{\text{FB}}^{0,\tau}$
m_Z	1.00	0.09	-0.01	0.01	-0.02	-0.01	0.02	0.06	0.04
Γ_Z	0.09	1.00	-0.14	0.00	-0.01	0.00	0.00	0.00	0.00
σ_h^0	-0.01	-0.14	1.00	0.07	0.12	0.08	0.01	0.00	0.00
R_e	0.01	0.00	0.07	1.00	0.05	0.04	-0.01	0.00	0.00
R_μ	-0.02	-0.01	0.12	0.05	1.00	0.05	-0.01	0.01	0.00
R_τ	-0.01	0.00	0.08	0.04	0.05	1.00	0.00	0.00	0.01
$A_{\text{FB}}^{0,e}$	0.02	0.00	0.01	-0.01	-0.01	0.00	1.00	0.01	0.01
$A_{\text{FB}}^{0,\mu}$	0.06	0.00	0.00	0.00	0.01	0.00	0.01	1.00	0.01
$A_{\text{FB}}^{0,\tau}$	0.04	0.00	0.00	0.00	0.00	0.01	0.01	0.01	1.00

Table 5: The correlation matrix for the set of parameters given in Table 4.

approximately to those of the four experiments combined. Comparison of the errors obtained in this way with those resulting from the normal fits allows the error components from the LEP energy uncertainty to be extracted. The result is insensitive to which of the experiments is used to provide the data. In order to check this method a global fit is performed to the hadronic cross-section data for all experiments for the years 1993, 1994 and 1995. This procedure takes all common errors into account without any approximations being necessary, and is therefore exact apart from the fact the data from earlier years and the leptonic channels are not taken into account yet in this procedure. The results agree with those of the first method.

If lepton universality is assumed, the set of 9 parameters given above is reduced to a set of 5 parameters. R_ℓ is defined as $R_\ell \equiv \Gamma_{\text{had}}/\Gamma_{\ell\ell}$, where $\Gamma_{\ell\ell}$ refers to the partial Z width for the decay into a pair of massless charged leptons.

The data of each of the four LEP experiments are consistent with lepton universality (the difference in χ^2 over the difference in d.o.f. with and without the assumption of lepton universality is 6/4, 4/4, 4/4 and 5/4 for ALEPH, DELPHI, L3 and OPAL, respectively). Table 6 provides the five parameters m_Z , Γ_Z , σ_h^0 , R_ℓ and $A_{\text{FB}}^{0,\ell}$ for the individual LEP experiments, assuming lepton universality. Tables 7 and 8 provide these five parameters and the corresponding correlation matrix for the combined result. Figure 1 shows, for each lepton species and for the combination assuming lepton universality, the resulting 68% probability contours in the R_ℓ - $A_{\text{FB}}^{0,\ell}$ plane. For completeness the partial decay widths of the Z boson are listed in Table 9.

	ALEPH	DELPHI	L3	OPAL
$m_Z(\text{GeV})$	91.1874 ± 0.0030	91.1859 ± 0.0028	91.1883 ± 0.0029	91.1822 ± 0.0039
$\Gamma_Z(\text{GeV})$	2.4948 ± 0.0047	2.4896 ± 0.0042	2.4996 ± 0.0043	2.4955 ± 0.0053
$\sigma_h^0(\text{nb})$	41.578 ± 0.083	41.566 ± 0.079	41.411 ± 0.074	41.53 ± 0.09
R_ℓ	20.766 ± 0.049	20.754 ± 0.068	20.788 ± 0.066	20.83 ± 0.06
$A_{\text{FB}}^{0,\ell}$	0.0187 ± 0.0017	0.0175 ± 0.0020	0.0187 ± 0.0026	0.0150 ± 0.0019
$\chi^2/\text{d.o.f.}$	200/221	178/161	144/163	15/10 ^(a)

Table 6: Line shape and asymmetry parameters from 5-parameter fits to the data of the four LEP experiments, assuming lepton universality. R_ℓ is defined as $R_\ell \equiv \Gamma_{\text{had}}/\Gamma_{\ell\ell}$, where $\Gamma_{\ell\ell}$ refers to the partial Z width for the decay into a pair of massless charged leptons.

^(a)This parameter set has been obtained by a parameter transformation applied to the 15 parameters of the OPAL fit.

Parameter	Average Value
$m_Z(\text{GeV})$	91.1863 ± 0.0020
$\Gamma_Z(\text{GeV})$	2.4946 ± 0.0027
$\sigma_h^0(\text{nb})$	41.508 ± 0.056
R_ℓ	20.778 ± 0.029
$A_{\text{FB}}^{0,\ell}$	0.0174 ± 0.0010

Table 7: Average line shape and asymmetry parameters from the results of the four LEP experiments given in Table 6, assuming lepton universality. R_ℓ is defined as $R_\ell \equiv \Gamma_{\text{had}}/\Gamma_{\ell\ell}$, where $\Gamma_{\ell\ell}$ refers to the partial Z width for the decay into a pair of massless charged leptons. The $\chi^2/\text{d.o.f.}$ of the average is 26/31.

	m_Z	Γ_Z	σ_h^0	R_ℓ	$A_{\text{FB}}^{0,\ell}$
m_Z	1.00	0.09	-0.01	-0.01	0.08
Γ_Z	0.09	1.00	-0.14	-0.01	0.00
σ_h^0	-0.01	-0.14	1.00	0.15	0.01
R_ℓ	-0.01	-0.01	0.15	1.00	0.01
$A_{\text{FB}}^{0,\ell}$	0.08	0.00	0.01	0.01	1.00

Table 8: The correlation matrix for the set of parameters given in Table 7.

Without Lepton Universality:		
Γ_{ee}	(MeV)	83.96 ± 0.15
$\Gamma_{\mu\mu}$	(MeV)	83.79 ± 0.22
$\Gamma_{\tau\tau}$	(MeV)	83.72 ± 0.26
With Lepton Universality:		
$\Gamma_{\ell\ell}$	(MeV)	83.91 ± 0.11
Γ_{had}	(MeV)	1743.6 ± 2.5
Γ_{inv}	(MeV)	499.5 ± 2.0

Table 9: Partial decay widths of the Z boson, derived from the results of the 9-parameter (Tables 4 and 5) and the 5-parameter fit (Tables 7 and 8). In the case of lepton universality, $\Gamma_{\ell\ell}$ refers to the partial Z width for the decay into a pair of massless charged leptons.

Preliminary

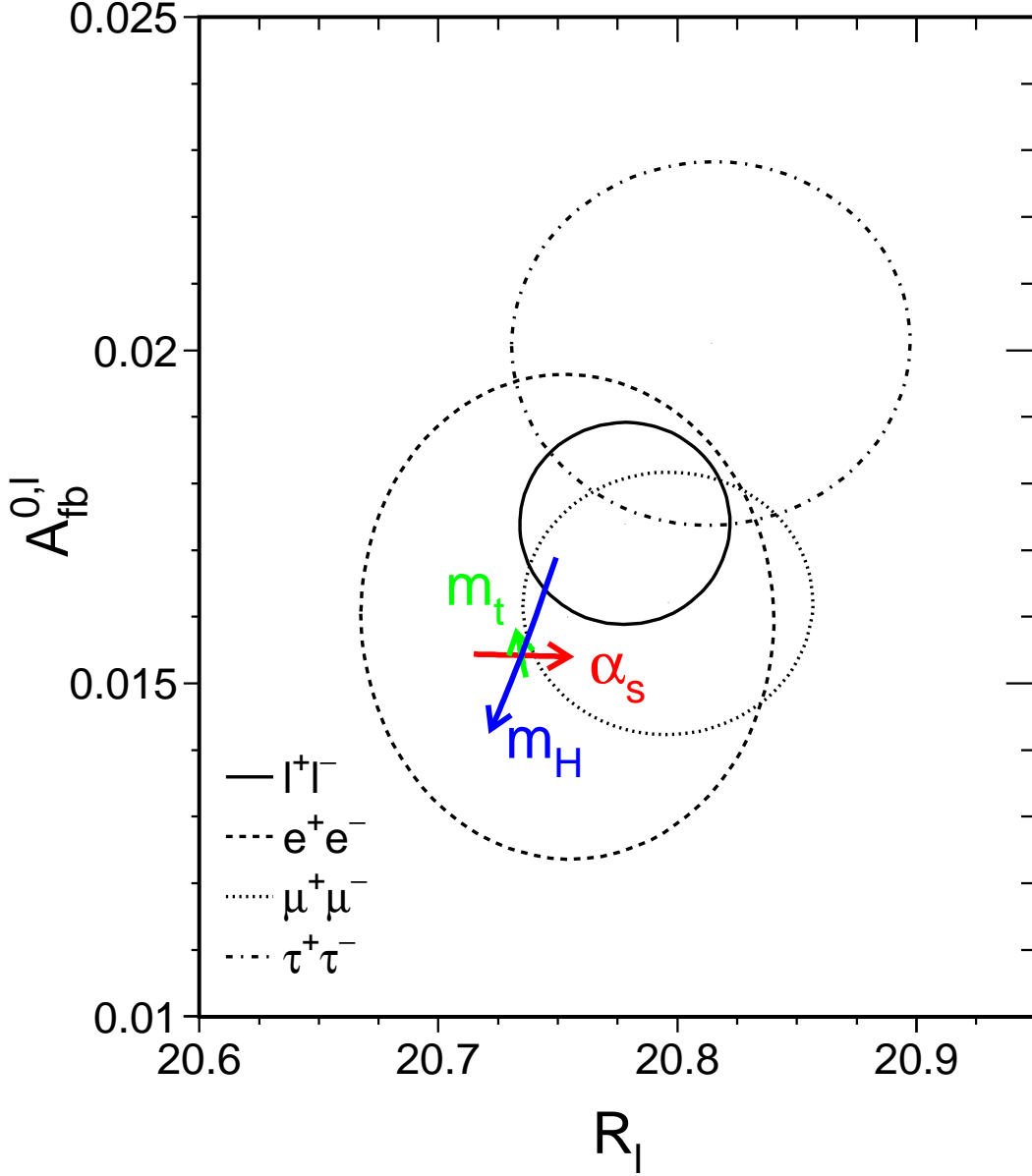


Figure 1: Contours of 68% probability in the R_ℓ - $A_{\text{FB}}^{0,\ell}$ plane. The Standard Model prediction for $m_Z = 91.1863$ GeV, $m_t = 175$ GeV, $m_H = 300$ GeV, and $\alpha_s(m_Z^2) = 0.118$ is also shown. The lines with arrows correspond to the variation of the Standard Model prediction when m_t , m_H or $\alpha_s(m_Z^2)$ are varied in the intervals $m_t = 175 \pm 6$ GeV, $m_H = 300_{-240}^{+700}$ GeV, and $\alpha_s(m_Z^2) = 0.118 \pm 0.003$, respectively. The arrows point in the direction of increasing values of m_t , m_H and α_s .

3 The τ Polarisation

Updates from last year:

Since the last note, DELPHI has included a preliminary analysis of the data from 1993 and 1994, and OPAL has finalized its 1990 – 1994 analysis.

The τ polarisation, \mathcal{P}_τ , is determined by a measurement of the longitudinal polarisation of τ pairs produced in Z decays. It is defined as:

$$\mathcal{P}_\tau \equiv \frac{\sigma_R - \sigma_L}{\sigma_R + \sigma_L}, \quad (4)$$

where σ_R and σ_L are the τ -pair cross sections for the production of a right-handed and left-handed τ^- , respectively. The angular distribution of \mathcal{P}_τ as a function of the angle θ between the e^- and the τ^- , for $\sqrt{s} = m_Z$, is given by:

$$\mathcal{P}_\tau(\cos \theta) = - \frac{\mathcal{A}_\tau(1 + \cos^2 \theta) + 2\mathcal{A}_e \cos \theta}{1 + \cos^2 \theta + 2\mathcal{A}_\tau \mathcal{A}_e \cos \theta}, \quad (5)$$

with \mathcal{A}_e and \mathcal{A}_τ as defined in Equation (3). Equation (5) neglects corrections for the effects of γ exchange, γZ interference and electromagnetic radiative corrections for initial- and final-state radiation. These effects are taken into account in the experimental analyses. In particular, these corrections account for the \sqrt{s} dependence of the tau polarisation, $\mathcal{P}_\tau(\cos \theta)$, which is important since the off-peak data are included in the event samples for all experiments. When averaged over all production angles \mathcal{P}_τ is a measurement of \mathcal{A}_τ . As a function of $\cos \theta$, $\mathcal{P}_\tau(\cos \theta)$ provides nearly independent determinations of both \mathcal{A}_τ and \mathcal{A}_e , thus allowing a test of the universality of the couplings of the Z to e and τ .

Each experiment makes separate \mathcal{P}_τ measurements using the five τ decay modes $e\nu\bar{\nu}$, $\mu\nu\bar{\nu}$, $\pi\nu$, $\rho\nu$ and $a_1\nu$ [16–19]. The $\rho\nu$ and $\pi\nu$ are the most sensitive channels, contributing weights of about 40% each in the average. DELPHI has also used an inclusive hadronic analysis. The combination is made of the results from each experiment already averaged over the τ decay modes.

3.1 Results

Tables 10 and 11 show the most recent results for \mathcal{A}_τ and \mathcal{A}_e obtained by the four experiments [16–19] and their combination. A study of the possible common systematic errors has shown these to be small [3] and thus no such errors have been included in the combination. The statistical correlation between the extracted values of \mathcal{A}_τ and \mathcal{A}_e is small ($\leq 5\%$), and is neglected.

The average values for \mathcal{A}_τ and \mathcal{A}_e :

$$\mathcal{A}_\tau = 0.1401 \pm 0.0067 \quad (6)$$

$$\mathcal{A}_e = 0.1382 \pm 0.0076, \quad (7)$$

are compatible, as is expected from lepton universality. Assuming $e-\tau$ universality, the values for \mathcal{A}_τ and \mathcal{A}_e can be combined. This combination is performed neglecting any possible common systematic error between \mathcal{A}_τ and \mathcal{A}_e within a given experiment, as these errors are also estimated to be small. The combined result of \mathcal{A}_τ and \mathcal{A}_e gives:

$$\mathcal{A}_\ell = 0.1393 \pm 0.0050. \quad (8)$$

ALEPH	('90 - '92), final	$0.136 \pm 0.012 \pm 0.009$
DELPHI	('90 - '94), prel.	$0.138 \pm 0.009 \pm 0.008$
L3	('90 - '94), prel.	$0.152 \pm 0.010 \pm 0.009$
OPAL	('90 - '94), final	$0.134 \pm 0.009 \pm 0.010$
LEP Average		0.1401 ± 0.0067

Table 10: LEP results for \mathcal{A}_τ . The $\chi^2/\text{d.o.f.}$ for the average is 1.1/3. The first error is statistical and the second systematic. In the LEP average, statistical and systematic errors are combined in quadrature. The systematic component of the error, obtained by combining the individual systematic errors (weighted by the total errors), is ± 0.0045 .

ALEPH	('90 - '92), final	$0.129 \pm 0.016 \pm 0.005$
DELPHI	('90 - '94), prel.	$0.140 \pm 0.013 \pm 0.003$
L3	('90 - '94), prel.	$0.156 \pm 0.016 \pm 0.005$
OPAL	('90 - '94), final	$0.129 \pm 0.014 \pm 0.005$
LEP Average		0.1382 ± 0.0076

Table 11: LEP results for \mathcal{A}_e . The $\chi^2/\text{d.o.f.}$ for the average is 1.8/3. The first error is statistical and the second systematic. In the LEP average, statistical and systematic errors are combined in quadrature. The systematic component of the error, obtained by combining the individual systematic errors (weighted by the total errors), is ± 0.0021 .

4 Results from b and c Quarks

Updates from last year:

Several new results on R_b are available, and there is an important change in the R_c analysis. In addition, the QCD correction for the asymmetries has been improved (see Section 4.2), and several measurements have been updated (see Section 4.4).

The relevant quantities in the heavy quark sector at LEP which are currently determined by the combination procedure are:

- The ratios³ of the b and c quark partial widths of the Z to its total hadronic partial width: $R_b^0 \equiv \Gamma_{b\bar{b}}/\Gamma_{\text{had}}$ and $R_c^0 \equiv \Gamma_{c\bar{c}}/\Gamma_{\text{had}}$.
- The forward-backward asymmetries, $A_{\text{FB}}^{b\bar{b}}$ and $A_{\text{FB}}^{c\bar{c}}$.
- The semileptonic branching ratios, $\text{BR}(b \rightarrow \ell)$ and $\text{BR}(b \rightarrow c \rightarrow \bar{\ell})$, and the average $B^0\bar{B}^0$ mixing parameter, $\bar{\chi}$. These are often determined at the same time as the widths or asymmetries in multi-parameter fits to lepton tag samples. They are included in the combination procedure to take into account their correlations with the other parameters measured in the same fit.
- The probability that a c-quark produces a D^{*+4} , a D^+ , a D_s or a charmed baryon. The probability that a c-quark fragments into a D^0 is calculated from the constraint that the probabilities for the weakly decaying charmed hadrons add up to one. These quantities are determined now with good accuracy by the LEP experiments. The interpretation of the D^* rate in terms of R_c and the determination of the charm background in the lifetime tag R_b measurements can now be made without assumptions on the energy dependence of the D-meson production rates.

There are several motivations for the averaging procedure [4] presented here. Several analyses measure more than one parameter simultaneously, for example the lepton fits. Some of the measurements of electroweak parameters depend explicitly on the values of other parameters, for example R_b depends on R_c . The common tagging and analysis techniques lead to common sources of systematic uncertainty, in particular for the double-tag measurements of R_b . The starting point for the combination is to ensure that all the analyses use a common set of assumptions for input parameters which give rise to systematic uncertainties. A full description of the averaging procedure has been published in Reference 4. The input parameters have been updated and extended recently [20] to accommodate new analyses and more recent measurements. The correlations and interdependences of the input measurements are then taken into account in a χ^2 minimisation which results in the combined electroweak parameters and their correlation matrix.

In a first fit the asymmetry measurements on peak, above peak and below peak were combined at each centre-of-mass energy. The results of this fit, including the SLD results, are given in the appendix. The dependence of the average asymmetries on centre-of-mass energy agrees with the prediction of the Standard Model. To derive the pole asymmetries, $A_{\text{FB}}^{0,q}$, from the measured quark asymmetries, all the off-peak asymmetry measurements were corrected to the peak energy before combining. Only results from this second fit are quoted here. There are therefore 11 parameters in total to be determined: the

³The symbols R_b^0 , R_c^0 denote the ratio of partial widths whereas R_b , R_c denote the experimentally measured ratios of cross sections ($R_b^0 = R_b + 0.0003$, $R_c^0 = R_c - 0.0003$).

⁴Actually the product $P(c \rightarrow D^{*+}) \times \text{BR}(D^{*+} \rightarrow \pi^+D^0)$ is fitted since this quantity is needed and measured by the LEP experiments.

two partial widths, two asymmetries, two semileptonic branching ratios, the average mixing parameter and the probabilities for c quark to fragment into a D^{*+} , a D^+ , a D_s , or a charmed baryon.

In addition the SLD collaboration has presented precise measurements of R_b [21] and of the left-right forward-backward asymmetry for b and c quarks [22]. Since the precision and the dominant sources of systematic uncertainty are similar at LEP and SLD it is useful to produce combined LEP+SLD averages. The left-right forward-backward asymmetries are, in contrast to the unpolarised forward-backward asymmetries, only sensitive to the final state couplings (\mathcal{A}_b and \mathcal{A}_c). They are treated in the averaging procedure as physically independent quantities. However the methods used to measure the polarised and unpolarised asymmetries are very similar, so \mathcal{A}_b and \mathcal{A}_c are included in the averaging procedure in order to estimate the correlation between the SLD and the LEP asymmetries, resulting in a 13-parameter fit.

4.1 Summary of measurements and averaging procedure

The measurements of R_b and R_c fall into two categories. In the first, called a single-tag measurement, a method to select b or c events is devised, and the number of tagged events is counted. This number must then be corrected for backgrounds from other flavours and for the tagging efficiency to calculate the true fraction of hadronic Z decays of that flavour. The dominant systematic errors come from understanding the branching ratios and detection efficiencies which give the overall tagging efficiency. For the second technique, called a double-tag measurement, the event is divided into two hemispheres. With N_t being the number of tagged hemispheres, N_{tt} the number of events with both hemispheres tagged and N_{had} the total number of hadronic Z decays one has:

$$\begin{aligned} \frac{N_t}{2N_{\text{had}}} &= \varepsilon_b R_b + \varepsilon_c R_c + \varepsilon_{\text{uds}}(1 - R_b - R_c), \\ \frac{N_{tt}}{N_{\text{had}}} &= C_b \varepsilon_b^2 R_b + C_c \varepsilon_c^2 R_c + C_{\text{uds}} \varepsilon_{\text{uds}}^2 (1 - R_b - R_c), \end{aligned}$$

where ε_b , ε_c and ε_{uds} are the tagging efficiencies per hemisphere for b, c and light-quark events, and $C_q \neq 1$ accounts for the fact that the tagging efficiencies between the hemispheres may be correlated. In the case of R_b one has $\varepsilon_b \gg \varepsilon_c \gg \varepsilon_{\text{uds}}$, $C_b \approx 1$. The correlations for the other flavours can be neglected. These equations can be solved to give R_b and ε_b . Neglecting the c and uds backgrounds and the correlations they are approximately given by:

$$\begin{aligned} \varepsilon_b &\approx 2N_{tt}/N_t, \\ R_b &\approx N_t^2/(4N_{tt}N_{\text{had}}). \end{aligned}$$

The double-tagging method has the advantage that the b tagging efficiency is derived directly from the data, reducing the systematic error of the measurement. The residual background of other flavours in the sample, and the evaluation of the correlation between the tagging efficiencies in the two hemispheres of the event are the main sources of systematic uncertainty in such an analysis.

The measurements included are:

- Lepton fits from all four LEP experiments [23–28]. These analyses use hadronic events with one or more leptons in the final state. Each analysis fits for several parameters chosen from R_b , R_c , $A_{\text{FB}}^{b\bar{b}}$, $A_{\text{FB}}^{c\bar{c}}$, $\text{BR}(b \rightarrow \ell)$ and $\text{BR}(b \rightarrow c \rightarrow \bar{\ell})$, and $\bar{\chi}$. Correlations exist between the different measured quantities, especially between R_b and $\text{BR}(b \rightarrow \ell)$. R_b and the semileptonic branching ratios are measured by a double-tagging technique where for the branching ratios the lepton

identification efficiency needs to be known. The dominant sources of systematic error for the lepton fits arise from the lepton identification, from other semileptonic branching ratios and from the modelling of the semileptonic decay. In addition to the single/double lepton fits ALEPH has measured $\text{BR}(b \rightarrow \ell)$ and $\text{BR}(b \rightarrow c \rightarrow \bar{\ell})$ in a lifetime tagged sample and R_c from low energy electrons assuming a value of $\text{BR}(c \rightarrow \ell)$.

- Event-shape tag for R_b from L3 (single tag) [29].
- Lifetime (and lepton) double tag measurements for R_b from ALEPH, DELPHI, L3, OPAL and SLD [21, 30–33]. These are the most precise determinations of R_b , and dominate the combined result. The basic features of the double-tag technique were discussed above. In the ALEPH and SLD measurements the charm rejection has been enhanced by using the invariant mass information. The ALEPH measurement makes use of five different tags; this improves the statistical accuracy and reduces the systematic errors due to hemisphere correlations and charm contamination, compared to the previous ALEPH analysis.
- Measurements of $A_{\text{FB}}^{b\bar{b}}$ based on lifetime tagged events with a hemisphere charge measurement from ALEPH, DELPHI and OPAL. The mean b-hemisphere charge is derived from the charge distributions themselves [26, 34, 35]. These measurements contribute roughly the same weight to the combined result as the lepton fits. Note that the quoted ALEPH result is a Standard Model fit to various charge properties both on- and off-peak which has been converted to an asymmetry determination.
- Analyses with $D/D^{*\pm}$ mesons to measure R_c from ALEPH, DELPHI and OPAL [24, 36, 37]. All measurements are constructed in a way that no assumptions on the energy dependence of charm fragmentation are necessary. The available measurements can be divided into four groups:
 - inclusive/exclusive double tag (ALEPH, DELPHI, OPAL): In a first step $D^{*\pm}$ mesons are reconstructed in several decay channels and their production rate is measured, which depends on the product $R_c \times P(c \rightarrow D^{*+}) \times \text{BR}(D^{*+} \rightarrow \pi^+ D^0)$. This sample of clean $c\bar{c}$ (and $b\bar{b}$) events is then used to measure $P(c \rightarrow D^{*+}) \times \text{BR}(D^{*+} \rightarrow \pi^+ D^0)$ using a slow pion tag in the opposite hemisphere. In the ALEPH measurement R_c is unfolded internally in the analysis so that no explicit $P(c \rightarrow D^{*+}) \times \text{BR}(D^{*+} \rightarrow \pi^+ D^0)$ is available. However the principle of the method is identical to the one of DELPHI and OPAL.
 - inclusive single/double tag (DELPHI): This measurement measures the single and double tag rate using a slow pion tag. It takes advantage of the much higher efficiency of the inclusive slow pion tag compared to the exclusive reconstruction. The high background, however, limits the precision of this measurement.
 - exclusive double tag (ALEPH): This analysis uses exclusively reconstructed D^{*+} , D^0 and D^+ mesons in different decay channels. It has lower statistics but much better purity than the inclusive analyses.
 - Reconstruction of all weakly decaying D states (DELPHI, OPAL): These analyses make the assumption that the production rates of D^0 , D^+ , D_s and Λ_c saturate the fragmentation of $c\bar{c}$ with small corrections applied for the unobserved baryonic states. This is a single tag measurement, relying only on knowing the decay branching ratios of the charm hadrons.
- Analyses with D mesons to measure $A_{\text{FB}}^{c\bar{c}}$ from ALEPH [38] or $A_{\text{FB}}^{c\bar{c}}$ and $A_{\text{FB}}^{b\bar{b}}$ from DELPHI and OPAL [26, 39].
- Measurements of \mathcal{A}_b and \mathcal{A}_c from SLD [22]. These results use lepton, kaon, D mesons and lifetime plus hemisphere charge tags, with similar sources of systematic error as the LEP asymmetry measurements.

These measurements are presented by the LEP and SLD collaborations in a consistent manner for the purpose of combination [4]. The tables prepared by the experiments include a detailed breakdown of the systematic error of each measurement and its dependence on other electroweak parameters. Where necessary, the experiments apply small corrections to their results in order to use agreed values and ranges for the input parameters to calculate systematic errors. The measurements, corrected where necessary, are summarised in the Appendix in Tables 24-33, where the statistical and systematic errors are quoted separately. The correlated systematic entries are from sources shared with one or more other results in the table and are derived from the full breakdown of common systematic uncertainties. The uncorrelated systematic entries come from the remaining sources.

A χ^2 minimisation procedure is used to derive the values of the heavy-flavour electroweak parameters as published in Reference 4. The full statistical and systematic covariance matrix for all measurements is calculated. This correlation matrix takes correlations between different measurements of one experiment and between different experiments into account. The explicit dependencies of each measurement on the other parameters are also accounted for. The most important example is the dependence of the value of R_b on the assumed value of R_c .

Since c-quark events form the main background in the R_b analyses, the value of R_b depends on the value of R_c . If R_b and R_c are measured in the same analysis, this is reflected in the correlation matrix for the results. However most analyses do not determine R_b and R_c simultaneously but instead measure R_b for an assumed value of R_c . In this case the dependence is parametrised as:

$$R_b = R_b^{\text{meas}} + a(R_c) \frac{(R_c - R_c^{\text{used}})}{R_c}. \quad (9)$$

In this expression, R_b^{meas} is the result of the analysis assuming a value of $R_c = R_c^{\text{used}}$. The values of R_c^{used} and the coefficients $a(R_c)$ are given in Table 24 where appropriate. The dependences of all other measurements on other electroweak parameters are treated in the same way, with coefficients $a(x)$ describing the dependence on parameter x .

4.2 Treatment of the LEP Asymmetry Measurements

For the 11- and 13-parameter fits described above, the peak and off-peak asymmetries were corrected to $\sqrt{s} = 91.26$ GeV using the predicted dependence from ZFITTER [40]. The slope of the asymmetry around m_Z depends only on the axial coupling and the charge of the initial and final state fermions and is thus independent of the value of the asymmetry itself.

After calculating the overall averages, the quark pole asymmetries, $A_{\text{FB}}^{0,q}$, were derived by applying the corrections described below. The measured asymmetries are all corrected to full acceptance. To relate the pole asymmetries to these numbers a few corrections that are summarised in Table 12 have to be applied. These corrections are the effects of the energy shift from 91.26 GeV to m_Z , initial state radiation, and γ exchange and γZ interference. All have been calculated using ZFITTER.

4.2.1 QCD corrections

The QCD corrections to the forward-backward asymmetries have been calculated in first [41] and second [42] order QCD. From these calculations a correction of $A_{\text{FB}}^{b,QCD} = (0.9689 \pm 0.0025) \times A_{\text{FB}}^{b,no\,QCD}$ has been estimated [20] for the b asymmetries, using the thrust axis as an estimate for the quark direction, but without experimental cuts. The error in the correction factor is mainly due to three

Source	$\delta A_{\text{FB}}^{\text{b}}$	$\delta A_{\text{FB}}^{\text{c}}$
$\sqrt{s} = m_Z$	-0.0013	-0.0034
QED corrections	+0.0041	+0.0104
$\gamma, \gamma Z$	-0.0003	-0.0008
Total	+0.0025	+0.0062

Table 12: Corrections to be applied to the quark asymmetries. The corrections are to be understood as $A_{\text{FB}}^0 = A_{\text{FB}}^{\text{meas}} + \sum_i (\delta A_{\text{FB}})_i$.

sources: the error on $\alpha_s(m_Z^2)$, the ambiguity in the renormalization scale and the uncertainty in the second order coefficient due to missing mass effects and a different definition of the event axis. In the past it has been assumed that whereas the lifetime/jet-charge measurements of asymmetries take into account these effects as an inherent part of the analysis, the measured asymmetries for the analyses using a lepton or D tag needed to be corrected by this amount. Experimental event selection and signal extraction, however, can introduce an important bias to the QCD corrections. In the case of the DELPHI measurement using a lepton tag, the QCD correction to the b (c) quark asymmetry has been estimated [20] to be reduced by 50% (70%) from its theoretical expectation. The effect of the lepton selection on the correction has been investigated by ALEPH and found to be smaller. The exact reasons of this difference and in particular the effect due to hadronization are presently under study. For the moment not all LEP experiments have estimated the effect of this bias on their measured asymmetries. For this reason, whenever an evaluation of the effect was not available, the measurements were corrected using the DELPHI estimation with an inflated error to take into account possible variations in the experimental bias. In these cases the correction factors used were 0.984 ± 0.008 for the b and 0.99 ± 0.01 for the c asymmetries. In the future, each experiment will perform the correction for their set of event selections.

As a consequence of this, all numbers given for $A_{\text{FB}}^{\text{b,c}}$ in the appendix are, if not stated otherwise, already corrected for QCD effects.

4.3 Results

4.3.1 Results of the 11-parameter fit to LEP data

Using the full averaging procedure gives the following combined results for the electroweak parameters:

$$\begin{aligned}
 R_{\text{b}}^0 &= 0.2179 \pm 0.0012 & (10) \\
 R_{\text{c}}^0 &= 0.1715 \pm 0.0056 \\
 A_{\text{FB}}^{0,\text{b}} &= 0.0979 \pm 0.0023 \\
 A_{\text{FB}}^{0,\text{c}} &= 0.0733 \pm 0.0049,
 \end{aligned}$$

where all corrections to the asymmetries and partial widths have been applied. The $\chi^2/\text{d.o.f.}$ is $50/(81 - 11)$. The corresponding correlation matrix is given in Table 13. If R_{c}^0 is fixed to its Standard Model prediction of 0.1723, then the value of R_{b}^0 is:

$$R_{\text{b}}^0(R_{\text{c}}^0 = 0.1723) = 0.2179 \pm 0.0011.$$

	R_b^0	R_c^0	$A_{\text{FB}}^{0,b}$	$A_{\text{FB}}^{0,c}$
R_b^0	1.00	-0.23	0.00	0.01
R_c^0	-0.23	1.00	0.04	-0.07
$A_{\text{FB}}^{0,b}$	0.00	0.04	1.00	0.10
$A_{\text{FB}}^{0,c}$	0.01	-0.07	0.10	1.00

Table 13: The reduced correlation matrix for the electroweak parameters from the 11-parameter fit.

4.3.2 Results of the 13-parameter fit to LEP and SLD data

Including the SLD results on R_b , \mathcal{A}_b and \mathcal{A}_c into the fit the following results are obtained:

$$\begin{aligned}
R_b^0 &= 0.2178 \pm 0.0011 \\
R_c^0 &= 0.1715 \pm 0.0056 \\
A_{\text{FB}}^{0,b} &= 0.0979 \pm 0.0023 \\
A_{\text{FB}}^{0,c} &= 0.0735 \pm 0.0048 \\
\mathcal{A}_b &= 0.863 \pm 0.049 \\
\mathcal{A}_c &= 0.625 \pm 0.084,
\end{aligned}
\tag{11}$$

with a $\chi^2/\text{d.o.f.}$ of $51/(87-13)$. The corresponding correlation matrix is given in Table 14. In deriving these results the parameters \mathcal{A}_b and \mathcal{A}_c have been treated as independent of the forward-backward asymmetries $A_{\text{FB}}^{b\bar{b}}(\text{pk})$ and $A_{\text{FB}}^{c\bar{c}}(\text{pk})$.

	R_b^0	R_c^0	$A_{\text{FB}}^{0,b}$	$A_{\text{FB}}^{0,c}$	\mathcal{A}_b	\mathcal{A}_c
R_b^0	1.00	-0.23	0.00	0.00	-0.03	0.01
R_c^0	-0.23	1.00	0.04	-0.06	0.05	-0.07
$A_{\text{FB}}^{0,b}$	0.00	0.04	1.00	0.10	0.04	0.02
$A_{\text{FB}}^{0,c}$	0.00	-0.06	0.10	1.00	0.01	0.10
\mathcal{A}_b	-0.03	0.05	0.04	0.01	1.00	0.12
\mathcal{A}_c	0.01	-0.07	0.02	0.10	0.12	1.00

Table 14: The reduced correlation matrix for the electroweak parameters from the 13-parameter fit.

If R_c^0 is fixed to its Standard Model prediction of 0.1723, then the value of R_b^0 is:

$$R_b^0(R_c^0 = 0.1723) = 0.2178 \pm 0.0011.$$

The result of the full fit to the LEP/SLC results including the off-peak asymmetries and the b semileptonic branching ratio can be found in the appendix. It should be noted that the result on $\text{BR}(b \rightarrow \ell)$ and the other non-electroweak parameters is independent of the treatment of the off-peak asymmetries and the SLD data.

4.4 Comments on the changes since last year

Compared to the results available last summer some changes occurred in the central values of R_b , R_c and $A_{\text{FB}}^{0,b}$.

For R_c a significant change comes from the fact that the low energy constraint on $P(c \rightarrow D^{*+})$ is no longer used. The low energy number $P(c \rightarrow D^{*+}) \times \text{BR}(D^{*+} \rightarrow \pi^+ D^0) = 0.178 \pm 0.013$ is consistent

with the LEP measurement of 0.163 ± 0.007 , but due to the large correlation of -60% (see table 23), R_c is pulled to 0.1637 when $P(c \rightarrow D^{*+}) \times BR(D^{*+} \rightarrow \pi^+ D^0)$ is fixed to 0.178. In addition all analyses have been improved and new data have been added. For the combined R_c result the largest errors are statistical (0.0037) and systematics internal to the experiments (0.0029). From the error sources common to the experiments the only relevant ones are the branching ratios $BR(c \rightarrow \ell)$ (0.0022) and $BR(D_s \rightarrow \phi\pi)$ (0.0011) for which the model independent CLEO measurement [43] is used. The branching ratio $BR(D^0 \rightarrow K\pi)$ contributes only 0.0002 to the total error on R_c . The CLEO measurement of this branching ratio is consistent with a recent ALEPH analysis [44].

Most of the change in R_b is due to the inclusion of new data. The new input parameters have the tendency to lower R_b as well, mainly due to the inclusion of the measured gluon splitting rate $g \rightarrow c\bar{c}$ [45]; however, this effect is only of the order 0.0003. The new data presented this summer are:

- ALEPH has presented a new analysis of their 1992 to 1995 data with a new very pure tag and a new multivariate technique.
- DELPHI has updated their number with 1994 data.
- L3 has now also presented a lifetime tag measurement.
- SLD has presented a new analysis using a very pure and efficient tag.

Since some of the R_b measurements depend on the charmed hadron production fractions which are also fitted parameters, it is no longer possible to fit simply the R_b measurements alone. To test the compatibility of these measurements the following procedure has been adopted: in a first step the LEP charm measurements have been combined to obtain a best estimate of the charm production fractions with R_c fixed to its Standard Model value. In a second step the precise single parameter R_b measurements have been fitted together with the result of the first fit. The result of this fit with R_c fixed to 0.172 was $R_b = 0.2174 \pm 0.0012$ with $\chi^2/\text{d.o.f.} = 5.1/5$ showing agreement between the different experiments. In addition the new ALEPH and DELPHI results are consistent with their older published numbers.

In addition R_b is lowered by about 0.0008 because of the change in R_c , as there is a -23% correlation between them.

For the combined R_b with R_c fixed, the dominant error sources are statistics (0.00067) and internal effects (0.00053). The dominant common effects are the inclusive branching ratio $D \rightarrow K^0 X$ (0.00022), the charged D decay multiplicity (0.00029), QCD related effects to the hemisphere correlations (0.00031) and the gluon splitting to b and c quark pairs (0.00044).

$A_{FB}^{0,b}$ is now 0.0018 lower than last year and the error has decreased by 25%. There are three equally important reasons for this change:

- the new OPAL lepton analysis,
- the ALEPH jet charge measurement,
- an improved treatment of the QCD corrections.

5 The Hadronic Charge Asymmetry $\langle Q_{\text{FB}} \rangle$

Updates from last year:

ALEPH has included the 1994 data and published their analysis. DELPHI has a new preliminary result, improving on their previous analysis and adding the 1992-1994 data.

The LEP experiments ALEPH [46–48], DELPHI [49, 50], and OPAL [51, 52] have provided measurements of the hadronic charge asymmetry based on the mean difference in jet charges measured in the forward and backward event hemispheres, $\langle Q_{\text{FB}} \rangle$. DELPHI has also provided a related measurement of the total charge asymmetry by making a charge assignment on an event-by-event basis and performing a likelihood fit [49]. The experimental values quoted for the average forward-backward charge difference, $\langle Q_{\text{FB}} \rangle$, cannot be directly compared as some of them include detector dependent effects such as acceptances and efficiencies. Therefore the effective electroweak mixing angle, $\sin^2\theta_{\text{eff}}^{\text{lept}}$, as defined in Section 6.3, is used as a means of combining the experimental results summarised in Table 15.

Experiment		$\sin^2\theta_{\text{eff}}^{\text{lept}}$
ALEPH	90-94, final	$0.2322 \pm 0.0008 \pm 0.0011$
DELPHI	91-94, prel.	$0.2311 \pm 0.0010 \pm 0.0014$
OPAL	91-94, prel.	$0.2326 \pm 0.0012 \pm 0.0013$
Average		0.2320 ± 0.0010

Table 15: Summary of the determination of $\sin^2\theta_{\text{eff}}^{\text{lept}}$ from inclusive hadronic charge asymmetries at LEP. For each experiment, the first error is statistical and the second systematic. The latter is dominated by fragmentation and decay modelling uncertainties.

The dominant source of systematic error arises from the modelling of the charge flow in the fragmentation process for each flavour. All experiments measure the required charge properties for $Z \rightarrow b\bar{b}$ events from the data. ALEPH also determines the charm charge properties from the data. The fragmentation model implemented in the JETSET Monte-Carlo program [53] is used by all experiments as reference; the one of the HERWIG Monte-Carlo program [54] is used for comparison. The JETSET fragmentation parameters are varied to estimate the systematic errors. The central values chosen by the experiments for these parameters are, however, not the same. The degree of correlation between the fragmentation uncertainties for the different experiments requires further investigation. The smaller of the two fragmentation errors in any pair of results is treated as common to both. The present average of $\sin^2\theta_{\text{eff}}^{\text{lept}}$ from $\langle Q_{\text{FB}} \rangle$ and its associated error are not very sensitive to the treatment of common uncertainties. The ambiguities due to QCD corrections may cause changes in the derived value of $\sin^2\theta_{\text{eff}}^{\text{lept}}$. These are, however, well below the fragmentation uncertainties and experimental errors. The effect of fully correlating the estimated systematic uncertainties from this source between the experiments has a negligible effect upon the average and its error.

There is also some correlation between these results and those for $A_{\text{FB}}^{b\bar{b}}$ using jet charges. The dominant source of correlation is again through uncertainties in the fragmentation and decay models used. The typical correlation between the derived values of $\sin^2\theta_{\text{eff}}^{\text{lept}}$ between the $\langle Q_{\text{FB}} \rangle$ and the $A_{\text{FB}}^{b\bar{b}}$ jet charge measurement has been estimated to be between 20% and 25%. This leads to only a small change in the relative weights for the $A_{\text{FB}}^{b\bar{b}}$ and $\langle Q_{\text{FB}} \rangle$ results when averaging their $\sin^2\theta_{\text{eff}}^{\text{lept}}$ values (Section 6.3). Furthermore, the jet charge method contributes at most half of the weight of the $A_{\text{FB}}^{b\bar{b}}$ measurement. Thus, the correlation between $\langle Q_{\text{FB}} \rangle$ and $A_{\text{FB}}^{b\bar{b}}$ from jet charge will have little impact on the overall Standard Model fit, and is neglected at present.

6 Interpretation of Results

Updates from last year:

The results of the Standard Model fit with the Higgs mass as a free parameter are presented.

6.1 The Coupling Parameters \mathcal{A}_f

The coupling parameters \mathcal{A}_f are defined in terms of the effective vector and axial-vector neutral current couplings of fermions (Equation (3)). The LEP measurements of the forward-backward asymmetries of charged leptons (Section 2) and b and c quarks (Section 4) determine the products $A_{\text{FB}}^{0,f} = \frac{3}{4}\mathcal{A}_e\mathcal{A}_f$ (Equation (2)). The LEP measurements of the τ polarisation (Section 3), $\mathcal{P}_\tau(\cos\theta)$, determine \mathcal{A}_τ and \mathcal{A}_e separately (Equation (5)). The SLD collaboration measures the left-right asymmetry, A_{LR} [55], which determines the same quantity, \mathcal{A}_e , as the τ polarisation, with minimal model dependence. Both measurements have small systematic errors. The SLD measurements of the left-right forward-backward asymmetries for b and c quarks [22] are direct determinations of \mathcal{A}_b and \mathcal{A}_c .

Table 16 shows the results for the leptonic coupling parameter \mathcal{A}_ℓ and their combination assuming lepton universality. The three results shown are all statistics dominated and the χ^2 of the combination (6 for 2 d.o.f) results in a probability of 4.7%. Table 17 shows the results on the quark coupling parameters \mathcal{A}_b and \mathcal{A}_c derived from LEP or SLD measurements separately (Equations 10 and 11) and from the combination of LEP and SLD measurements (Equation 11). It should be noted that the combined LEP+SLD measurement of \mathcal{A}_b is about 3 standard deviations below the Standard Model prediction (0.935, see Table 20). This is due to three independent circumstances: the SLD measurement of \mathcal{A}_b is low compared to the Standard Model; the LEP measurement of $A_{\text{FB}}^{0,b}$ is low; and the SLD measurement of A_{LR} is high compared to the Standard Model.

	\mathcal{A}_ℓ	Cumulative Average	$\chi^2/\text{d.o.f.}$
$A_{\text{FB}}^{0,\ell}$	0.1523 ± 0.0044		
$\mathcal{P}_\tau(\cos\theta)$	0.1393 ± 0.0050	0.1466 ± 0.0033	3.8/1
A_{LR} (SLD)	0.1542 ± 0.0037	0.1500 ± 0.0025	6.1/2

Table 16: Comparison of the determinations of the leptonic coupling parameter \mathcal{A}_ℓ assuming lepton universality. The second column lists the \mathcal{A}_ℓ values derived from the quantities listed in the first column. The third column contains the cumulative averages of these \mathcal{A}_ℓ results. The averages are derived assuming no correlations between the measurements. The χ^2 per degree of freedom for the cumulative averages is given in the last column.

	LEP ($\mathcal{A}_\ell = 0.1466 \pm 0.0033$)	SLD	LEP+SLD ($\mathcal{A}_\ell = 0.1500 \pm 0.0025$)
\mathcal{A}_b	0.890 ± 0.029	0.863 ± 0.049	0.867 ± 0.022
\mathcal{A}_c	0.667 ± 0.047	0.625 ± 0.084	0.646 ± 0.040

Table 17: Determinations of the quark coupling parameters \mathcal{A}_b and \mathcal{A}_c from LEP data alone (using the LEP average for \mathcal{A}_ℓ), from SLD data alone, and from LEP+SLD data (using the LEP+SLD average for \mathcal{A}_ℓ) assuming lepton universality.

6.2 The Effective Vector and Axial-Vector Coupling Constants

The partial widths of the Z into leptons and the lepton forward-backward asymmetries (Section 2), the τ polarisation and the τ polarisation asymmetry (Section 3) can be combined to determine the effective vector and axial-vector couplings for e, μ and τ . The asymmetries (Equations (2) and (5)) determine the ratio $g_{V\ell}/g_{A\ell}$ (Equation (3)), while the sum of the squares of the couplings is derived from the leptonic partial widths:

$$\Gamma_{\ell\ell} = \frac{G_F m_Z^3}{6\pi\sqrt{2}} (g_{V\ell}^2 + g_{A\ell}^2) (1 + \delta_\ell^{QED}), \quad (12)$$

where $\delta_\ell^{QED} = 3q_\ell^2\alpha(m_Z^2)/(4\pi)$ accounts for final state photonic corrections. Corrections due to lepton masses, neglected in Equation 12, are taken into account for the results presented below.

The averaged results for the effective lepton couplings are given in Table 18. Figure 2 shows the 68% probability contours in the $g_{A\ell}$ - $g_{V\ell}$ plane. The signs of $g_{A\ell}$ and $g_{V\ell}$ are based on the convention $g_{Ae} < 0$. With this convention the signs of the couplings of all charged leptons follow from LEP data alone. For comparison, the $g_{V\ell}$ - $g_{A\ell}$ relation following from the measurement of A_{LR} from SLD [55] is indicated as a band in the $g_{A\ell}$ - $g_{V\ell}$ -plane of Figure 2. It is consistent with the LEP data. The information on the leptonic couplings from LEP can therefore be combined with the A_{LR} measurement of SLD. The results for this combination are given in the right column of Table 18. The measured ratios of the e, μ and τ couplings provide a test of lepton universality and are also given in Table 18.

	Without Lepton Universality:	
	LEP	LEP+SLD
g_{Ve}	-0.0368 ± 0.0015	-0.03828 ± 0.00079
$g_{V\mu}$	-0.0372 ± 0.0034	-0.0358 ± 0.0030
$g_{V\tau}$	-0.0369 ± 0.0016	-0.0367 ± 0.0016
g_{Ae}	-0.50130 ± 0.00046	-0.50119 ± 0.00045
$g_{A\mu}$	-0.50076 ± 0.00069	-0.50086 ± 0.00068
$g_{A\tau}$	-0.50116 ± 0.00079	-0.50117 ± 0.00079
	Ratios of couplings:	
	LEP	LEP+SLD
$g_{V\mu}/g_{Ve}$	1.01 ± 0.11	0.935 ± 0.085
$g_{V\tau}/g_{Ve}$	1.001 ± 0.062	0.959 ± 0.046
$g_{A\mu}/g_{Ae}$	0.9989 ± 0.0018	0.9993 ± 0.0017
$g_{A\tau}/g_{Ae}$	0.9997 ± 0.0019	1.0000 ± 0.0019
	With Lepton Universality:	
	LEP	LEP+SLD
$g_{V\ell}$	-0.03688 ± 0.00085	-0.03776 ± 0.00062
$g_{A\ell}$	-0.50115 ± 0.00034	-0.50108 ± 0.00034
g_ν	$+0.5009 \pm 0.0010$	$+0.5009 \pm 0.0010$

Table 18: Results for the effective vector and axial-vector couplings derived from the combined LEP data without and with the assumption of lepton universality. For the right column the SLD measurement of A_{LR} is also included.

The neutrino couplings to the Z can be derived from the measured value of its invisible width, Γ_{inv} , attributing it exclusively to the decay into three identical neutrino generations ($\Gamma_{\text{inv}} = 3\Gamma_{\nu\nu}$) and assuming $g_{A\nu} \equiv g_{V\nu} \equiv g_\nu$. The relative sign of g_ν is chosen to be in agreement with neutrino scattering data [56], resulting in $g_\nu = +0.5009 \pm 0.0010$.

Preliminary

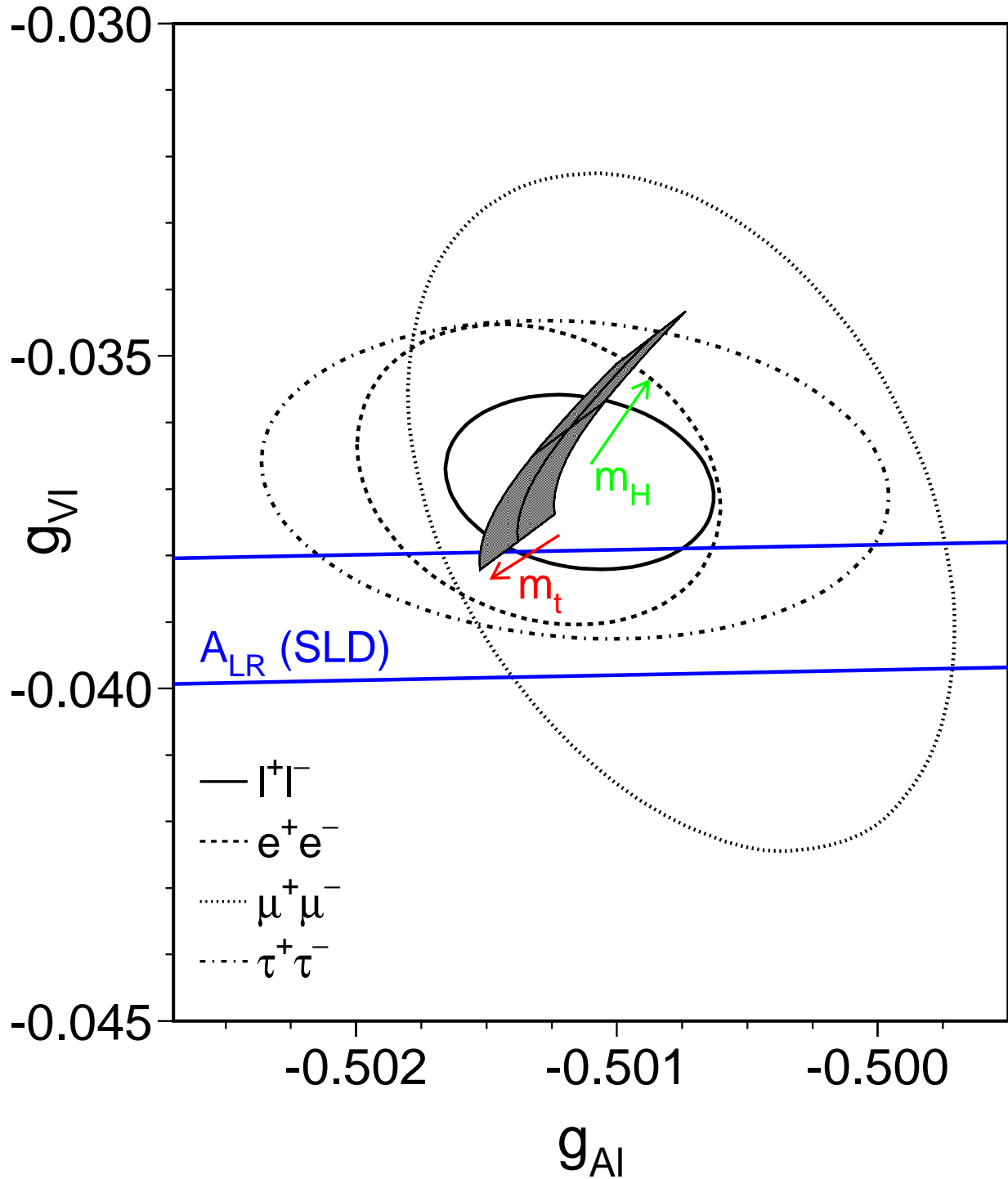


Figure 2: Contours of 68% probability in the $g_{V\ell}$ - $g_{A\ell}$ plane from LEP measurements. The solid contour results from a fit assuming lepton universality. Also shown is the one standard deviation band resulting from the A_{LR} measurement of SLD. The shaded region corresponds to the Standard Model prediction for $m_t = 175 \pm 6$ GeV and $m_H = 300^{+700}_{-240}$ GeV. The arrows point in the direction of increasing values of m_t and m_H .

6.3 The Effective Electroweak Mixing Angle $\sin^2\theta_{\text{eff}}^{\text{lept}}$

The asymmetry measurements from LEP can be combined into a single observable, the effective electroweak mixing angle, $\sin^2\theta_{\text{eff}}^{\text{lept}}$, defined as:

$$\sin^2\theta_{\text{eff}}^{\text{lept}} \equiv \frac{1}{4}(1 - g_{V\ell}/g_{A\ell}), \quad (13)$$

without making any strong model-specific assumptions.

For a combined average of $\sin^2\theta_{\text{eff}}^{\text{lept}}$ from $A_{\text{FB}}^{0,\ell}$, \mathcal{A}_τ and \mathcal{A}_e only the assumption of lepton universality, already inherent in the definition of $\sin^2\theta_{\text{eff}}^{\text{lept}}$, is needed. In practice no further assumption is involved if the quark forward-backward asymmetries, $A_{\text{FB}}^{0,b}$ and $A_{\text{FB}}^{0,c}$, are included in this average, as these asymmetries have a reduced sensitivity to corrections particular to the hadronic vertex. The results of these determinations of $\sin^2\theta_{\text{eff}}^{\text{lept}}$ and their combination are shown in Table 19. Also the measurement of the left-right asymmetry, A_{LR} , from SLD [55] is given. Compared to the results presented in our previous note [1], the χ^2 of the average of all determinations has increased by 5. The most significant change in central value is for $A_{\text{FB}}^{0,b}$, although it is consistent within errors with the previous result. The errors on most results have decreased considerably.

	$\sin^2\theta_{\text{eff}}^{\text{lept}}$	Average by Group of Observations	Cumulative Average	$\chi^2/\text{d.o.f.}$
$A_{\text{FB}}^{0,\ell}$	0.23085 ± 0.00056			
\mathcal{A}_τ	0.23240 ± 0.00085			
\mathcal{A}_e	0.23264 ± 0.00096	0.23157 ± 0.00042	0.23157 ± 0.00042	3.9/2
$A_{\text{FB}}^{0,b}$	0.23246 ± 0.00041			
$A_{\text{FB}}^{0,c}$	0.23155 ± 0.00112	0.23236 ± 0.00038	0.23200 ± 0.00028	6.3/4
$\langle Q_{\text{FB}} \rangle$	0.2320 ± 0.0010	0.2320 ± 0.0010	0.23200 ± 0.00027	6.3/5
A_{LR} (SLD)	0.23061 ± 0.00047	0.23061 ± 0.00047	0.23165 ± 0.00024	12.8/6

Table 19: Comparison of several determinations of $\sin^2\theta_{\text{eff}}^{\text{lept}}$ from asymmetries. Averages are obtained as weighted averages assuming no correlations. The second column lists the $\sin^2\theta_{\text{eff}}^{\text{lept}}$ values derived from the quantities listed in the first column. The third column contains the averages of these numbers by groups of observations, where the groups are separated by the horizontal lines. The last column shows the cumulative averages. The χ^2 per degree of freedom for the cumulative averages is also given.

6.4 Number of Neutrino Species

An important aspect of our measurement concerns the information related to Z decays into invisible channels. Using the results of Tables 7 and 8, the ratio of the Z decay width into invisible particles and the leptonic decay width is determined:

$$\Gamma_{\text{inv}}/\Gamma_{\ell\ell} = 5.952 \pm 0.023.$$

The Standard Model value for the ratio of the partial widths to neutrinos and charged leptons is:

$$(\Gamma_{\nu\nu}/\Gamma_{\ell\ell})_{\text{SM}} = 1.991 \pm 0.001.$$

The central value is evaluated for $m_Z = 91.1863$ GeV, $m_t = 175$ GeV, $m_H = 300$ GeV and the error quoted accounts for a variation of m_t in the range $m_t = 175 \pm 6$ GeV and a variation of m_H in the range $60 \text{ GeV} \leq m_H \leq 1000 \text{ GeV}$.

The number of light neutrino species is given by the ratio of the two expressions listed above:

$$N_\nu = 2.989 \pm 0.012.$$

6.5 Constraints on the Standard Model

The precise electroweak measurements performed at LEP can be used to check the validity of the Standard Model and, within its framework, to infer valuable information about its fundamental parameters. The accuracy of the measurements makes them sensitive to the top-quark mass, m_t , and to the mass of the Higgs boson, m_H , through loop corrections. The leading m_t dependence is quadratic and allows a determination of m_t . The main dependence on m_H is logarithmic and therefore, with the present experimental precision, the constraints on m_H are still weak.

The LEP measurements used are summarised in Table 20a together with the Standard Model predictions. Also shown are the results from the SLD collaboration [21,22,55] as well as measurements of m_W from UA2 [65], CDF [66,67], and DØ [68]⁵, measurements of the neutrino neutral to charged current ratios from CDHS [59], CHARM [60] and CCFR [61], and the measurement of the top quark mass [62–64] by CDF and DØ. In addition, the determination of the electromagnetic coupling constant, $\alpha(m_Z^2)$, which is used in the fits, is shown. An additional input parameter, not shown in the table, is the Fermi constant, G_F , determined from the muon lifetime, $G_F = 1.16639 \times 10^{-5} \text{ GeV}^{-2}$ [69].

Detailed studies of the theoretical uncertainties in the Standard Model predictions due to missing higher-order electroweak corrections and their interplay with QCD corrections are carried out in the working group on ‘Precision calculations for the Z resonance’ [70]. Theoretical uncertainties are evaluated by comparing different but, within our present knowledge, equivalent treatments of aspects such as resummation techniques, momentum transfer scales for vertex corrections and factorisation schemes. The impact of these intrinsic theoretical uncertainties on m_t and $\alpha_s(m_Z^2)$ has been estimated by repeating the Standard Model fits in this Section using several combinations of options which were implemented in the electroweak libraries used [71] for the study performed in Reference 70. As a result the maximal variations of the central values of the fitted parameters correspond to an additional theoretical error of less than 1 GeV on m_t , less than 0.001 on $\alpha_s(m_Z^2)$ and 0.1 on $\log(m_H)$. Although the theoretical error on $\log(m_H)$ is still smaller than the experimental error, it is relatively more important than the theoretical error on m_t or $\alpha_s(m_Z^2)$. More studies on the effect would be welcome. The theoretical error on $\alpha_s(m_Z^2)$ covers missing higher-order electroweak corrections and uncertainties in the interplay of electroweak and QCD corrections. The effect of missing higher-order QCD corrections on $\alpha_s(m_Z^2)$ is estimated to be about 0.002 [72]. A discussion of theoretical uncertainties in the determination of α_s can be found in References 70 and 72. All theoretical errors discussed in this paragraph have been neglected for the results presented in Tables 21 and 22.

At present the impact of theoretical uncertainties on the determination of m_t from precise electroweak measurements is small compared to the error due to the uncertainty in the value of $\alpha(m_Z^2)$. The uncertainty in $\alpha(m_Z^2)$ arises from the contribution of light quarks to the photon vacuum polarisation. Recently there have been several reevaluations of $\alpha(m_Z^2)$ [57, 73–75]. For the results presented in this Section, a value of $\alpha(m_Z^2) = 1/(128.896 \pm 0.090)$ [57] is used. This uncertainty causes an error

⁵See Reference 58 for a combination of these m_W measurements.

	Measurement with Total Error	Systematic Error	Standard Model	Pull
$\alpha(m_Z^2)^{-1}$ [57]	128.896 ± 0.090	0.083	128.907	-0.1
a) <u>LEP</u> line-shape and lepton asymmetries: m_Z [GeV] Γ_Z [GeV] σ_h^0 [nb] R_ℓ $A_{\text{FB}}^{0,\ell}$ + correlation matrix Table 8 τ polarisation: \mathcal{A}_τ \mathcal{A}_e b and c quark results: $R_b^{0(b)}$ $R_c^{0(b)}$ $A_{\text{FB}}^{0,b(b)}$ $A_{\text{FB}}^{0,c(b)}$ + correlation matrix Table 13 $q\bar{q}$ charge asymmetry: $\sin^2\theta_{\text{eff}}^{\text{lept}}$ ((Q_{FB}))	91.1863 ± 0.0020 2.4946 ± 0.0027 41.508 ± 0.056 20.778 ± 0.029 0.0174 ± 0.0010 0.1401 ± 0.0067 0.1382 ± 0.0076 0.2179 ± 0.0012 0.1715 ± 0.0056 0.0979 ± 0.0023 0.0733 ± 0.0049 0.2320 ± 0.0010	$^{(a)}0.0015$ $^{(a)}0.0017$ 0.055 0.024 0.007 0.0045 0.0021 0.0009 0.0042 0.0010 0.0026 0.0008	91.1861 2.4960 41.465 20.757 0.0159 0.1458 0.1458 0.2158 0.1723 0.1022 0.0730 0.23167	0.1 -0.5 0.8 0.7 1.4 -0.9 -1.0 1.8 -0.1 -1.8 0.1 0.3
b) <u>SLD</u> $\sin^2\theta_{\text{eff}}^{\text{lept}}$ (A_{LR} [55]) R_b^0 [21] ^(b) \mathcal{A}_b [22] \mathcal{A}_c [22]	0.23061 ± 0.00047 0.2149 ± 0.0038 0.863 ± 0.049 0.625 ± 0.084	0.00014 0.0021 0.032 0.041	0.23167 0.2158 0.935 0.667	-2.2 -0.2 -1.4 -0.5
c) <u>p\bar{p} and νN</u> m_W [GeV] (p \bar{p} [58]) $1 - m_W^2/m_Z^2$ (νN [59-61]) m_t [GeV] (p \bar{p} [62-64])	80.356 ± 0.125 0.2244 ± 0.0042 175 ± 6	0.110 0.0036 4.5	80.353 0.2235 172	0.0 0.2 0.5

Table 20: Summary of measurements included in the combined analysis of Standard Model parameters. Section a) summarises LEP averages, Section b) SLD results for $\sin^2\theta_{\text{eff}}^{\text{lept}}$ from the measurement of the left-right polarisation asymmetry, for R_b and for \mathcal{A}_b and \mathcal{A}_c from polarised forward-backward asymmetries and Section c) electroweak precision measurements from p \bar{p} colliders and νN scattering. The total errors in column 2 include the systematic errors listed in column 3. The determination of the systematic part of each error is approximate. The Standard Model results in column 4 and the pulls (difference between measurement and fit in units of the total measurement error) in column 5 are derived from the Standard Model fit including all data (Table 22, column 3) with the Higgs mass treated as a free parameter.

^(a)The systematic errors on m_Z and Γ_Z contain the errors arising from the uncertainties in the LEP energy only.

^(b)For fits which combine LEP and SLD heavy flavour measurements we use as input the heavy flavour results given in Equation (11) and their correlation matrix in Table 14 in Section 4 of this note.

	LEP	LEP + SLD	LEP + SLD + p \bar{p} and ν N data
m_t (GeV)	$171 \pm 8 \begin{smallmatrix} +17 \\ -19 \end{smallmatrix}$	$177 \begin{smallmatrix} +7 \\ -8 \end{smallmatrix} \begin{smallmatrix} +17 \\ -19 \end{smallmatrix}$	$177 \pm 7 \begin{smallmatrix} +16 \\ -19 \end{smallmatrix}$
$\alpha_s(m_Z^2)$	$0.122 \pm 0.003 \pm 0.002$	$0.121 \pm 0.003 \pm 0.002$	$0.121 \pm 0.003 \pm 0.002$
$\chi^2/\text{d.o.f.}$	10/9	20/12	20/14

Table 21: Results of fits to LEP and other electroweak precision data for m_t and $\alpha_s(m_Z^2)$. No external constraint on $\alpha_s(m_Z^2)$ has been imposed. The first column presents the results obtained using LEP data only (Table 20a). The second column gives the result when the SLD measurements of the left-right asymmetry and electroweak heavy flavour results (Table 20b) are also added. In the third column also the combined data from p \bar{p} colliders and ν N experiments (Table 20c except m_t) are included. The central values and the first errors quoted refer to $m_H = 300$ GeV. The second errors correspond to the variation of the central value when varying m_H in the interval $60 \text{ GeV} \leq m_H \leq 1000 \text{ GeV}$. See text for a discussion of theoretical errors not included in the errors above.

of 0.00023 on the Standard Model prediction of $\sin^2\theta_{\text{eff}}^{\text{lept}}$, and an error of 4 GeV on m_t (for fixed m_H), which are included in the results listed in Table 21. The effect on the Standard Model prediction for $\Gamma_{\ell\ell}$ is negligible. The $\alpha_s(m_Z^2)$ values for the Standard Model fits presented in this Section are stable against a variation of $\alpha(m_Z^2)$ in the interval quoted. For the fits with the Higgs mass left free (see Table 22), the error is 1 GeV on m_t and 0.2 on $\log(m_H)$, which are also included in the results.

Table 21 shows the constraints obtained on m_t and $\alpha_s(m_Z^2)$ when fitting the measurements in Table 20 to up-to-date Standard Model calculations [71]. The fits have been repeated for $m_H = 60, 300$ and 1000 GeV and the difference in the fitted parameters is quoted as the second uncertainty. The results obtained using only LEP data (Table 20a), as well as those obtained by including preliminary results from the SLD collaboration (Table 20b) are shown in Table 21. The right-most column of Table 21 gives the Standard Model constraints obtained by including in addition the results given in Table 20c, except for the m_t result.

The $\chi^2/\text{d.o.f.}$ values for all these fits have probabilities ranging from 6% to 33%. In our previous report [1], the measurements of R_b and R_c contributed a χ^2 of approximately 15 for all the Standard Model fits in Table 21. For the new data set reported here the situation has changed significantly and the contributed χ^2 has reduced to approximately 3 (see Table 20 and Figure 3).

Figure 4 shows a comparison of the leptonic partial width from LEP (Table 9) and the effective electroweak mixing angle from asymmetries measured at LEP and SLD (Table 19), with the Standard Model. Good agreement with the Standard Model prediction is observed. The star shows the prediction if, among the electroweak radiative corrections only the photon vacuum polarisation is included, showing evidence that LEP/SLD data are sensitive to genuine electroweak corrections. Note that the error due to the uncertainty on $\alpha(m_Z^2)$ (shown as the length of the arrow attached to the star) is as large as the experimental error on $\sin^2\theta_{\text{eff}}^{\text{lept}}$ from LEP and SLD.

The value of $\alpha_s(m_Z^2)$ derived from an analysis of electroweak precision tests within the Standard Model framework depends essentially on R_ℓ , Γ_Z and σ_h^0 . The result is in very good agreement with the world average ($\alpha_s(m_Z^2) = 0.118 \pm 0.003$ [69]) and is of similar precision. The strong coupling constant can also be determined from the parameter R_ℓ alone. For $m_Z = 91.1863$ GeV, and imposing $m_t = 175 \pm 6$ GeV as a constraint, $\alpha_s = 0.124 \pm 0.004 \pm 0.002$ is obtained, where the second error accounts for the variation of the result when varying m_H in the range $60 \text{ GeV} \leq m_H \leq 1000 \text{ GeV}$.

In Figure 5 the fitted result for R_b with R_c fixed to its Standard Model value is plotted versus $\sin^2\theta_{\text{eff}}^{\text{lept}}$. If one assumes the Standard Model dependence of the partial widths on $\sin^2\theta_{\text{eff}}^{\text{lept}}$ for the light quarks and the c quark, and takes $\alpha_s(m_Z^2) = 0.118 \pm 0.003$, R_ℓ imposes a constraint on the two variables. A good agreement is seen for these 3 experimentally independent measurements, showing the consistency of the LEP data.

The fitted value of m_t is in excellent agreement with the top mass value $m_t = 175 \pm 6$ GeV reported [62–64] by the CDF and DØ collaborations. Note, however, that there is a large correlation between the top mass and the Higgs mass. This can be easily seen in the large variation (36 GeV) of the top mass when changing the Higgs mass between 60 and 1000 GeV. This large correlation is due to the fact that most of the observables listed in Table 20 are sensitive to both m_t and m_H . With the direct measurement of m_t that is now available, it should be possible to constrain m_H .

To constrain m_H , we first perform a fit to the LEP data alone as in Table 21, but fitting as well the Higgs mass. The result is shown in Table 22, column 2. This fit shows that the LEP data prefer a light top quark and a light Higgs, albeit with very large errors. The strongly asymmetric errors on m_H are due to the fact that to first order, the radiative corrections in the Standard Model are proportional to $\log(m_H)$. The correlation between the top quark mass and the Higgs mass is 0.78. It should be noted that the correlation would be even larger if the R_b measurement is not used, as R_b is insensitive to m_H . We then perform a second fit to all data, including the TEVATRON top mass result, which is shown in column 3 of Table 22. As can be expected, both m_t and m_H increase. The correlation between m_t and m_H is reduced somewhat to 0.64. This can also be seen in Figure 6 which shows the contours in m_t and m_H for these two fits. In Figures 7 and 8 the sensitivity of the LEP measurements to the Higgs mass is shown. As can be seen, the most sensitive measurements are the asymmetries. (This is also visible in Figure 4.) A reduced uncertainty for the value of $\alpha(m_Z^2)$ would therefore result in an improved constraint on m_H .

	LEP	LEP +SLD + p \bar{p} and ν N data + m_t
m_t [GeV]	155_{-13}^{+18}	172 ± 6
m_H [GeV]	86_{-51}^{+202}	149_{-82}^{+148}
$\log(m_H)$	$1.93_{-0.39}^{+0.52}$	$2.17_{-0.35}^{+0.30}$
$\alpha_s(m_Z^2)$	0.121 ± 0.003	0.120 ± 0.003
$\chi^2/\text{d.o.f.}$	9/8	19/14
$\sin^2\theta_{\text{eff}}^{\text{lept}}$	0.23198 ± 0.00026	0.23167 ± 0.00023
$1 - m_W^2/m_Z^2$	0.2249 ± 0.0009	0.2235 ± 0.0006
m_W (GeV)	80.278 ± 0.049	80.352 ± 0.033

Table 22: Results of the fits to LEP data alone and to all data including the top quark mass determination. As the sensitivity to m_H is logarithmic, both m_H as well as $\log(m_H)$ are quoted. The bottom part of the table lists derived results for $\sin^2\theta_{\text{eff}}^{\text{lept}}$, $1 - m_W^2/m_Z^2$ and m_W . See text for a discussion of theoretical errors not included in the errors above.

In Figure 9 the observed value of $\Delta\chi^2 \equiv \chi^2 - \chi_{\text{min}}^2$ as a function of m_H is plotted for the fit shown including the CDF/DØ m_t measurement. The shaded band shows the additional error due to the missing higher order corrections. Taking this error into account yields the one-sided 95% confidence level upper limit on m_H of 550 GeV. The lower limit on m_H of 66 GeV obtained from direct searches [76] has not been used in this limit determination.

7 Prospects for the Future

The LEP energy has now been increased; the Z phase of LEP has come to an end. However, the analyses of the data are far from finished. The major improvements which should happen in the near future will be:

- completion of the lineshape analysis, including final LEP energy calibrations. The biggest improvement should be in the measurement of Γ_Z ;
- improved measurements of R_b using new techniques;
- completion of the τ polarisation measurements, especially of the statistics dominated measurement of \mathcal{A}_e ;
- the errors on the measurements from SLD (A_{LR} , R_b , \mathcal{A}_b and \mathcal{A}_c) should decrease by a factor of 1.4 to 2

In addition, the measurements of m_W at both the TEVATRON and LEP II [77] will begin to match the error obtained via the radiative corrections of the Z data, and will provide a further important test of the Standard Model.

8 Conclusions

The combination of the many precise electroweak results yields stringent constraints on the Standard Model. All LEP measurements agree well with the predictions. Including all measurements, the data show some sensitivity to the Higgs mass.

The LEP experiments wish to stress that this report reflects a preliminary status at the time of the 1996 summer conferences. A definitive statement on these results has to wait for publication by each collaboration.

Acknowledgements

We would like to thank the SL Division of CERN for the efficient operation of the LEP accelerator, the precise information on the absolute energy scale and their close cooperation with the four experiments. We would also like to thank members of the CDF, DØ and SLD Collaborations for making results available to us in advance of the conferences and for useful discussions concerning their combination.

Preliminary

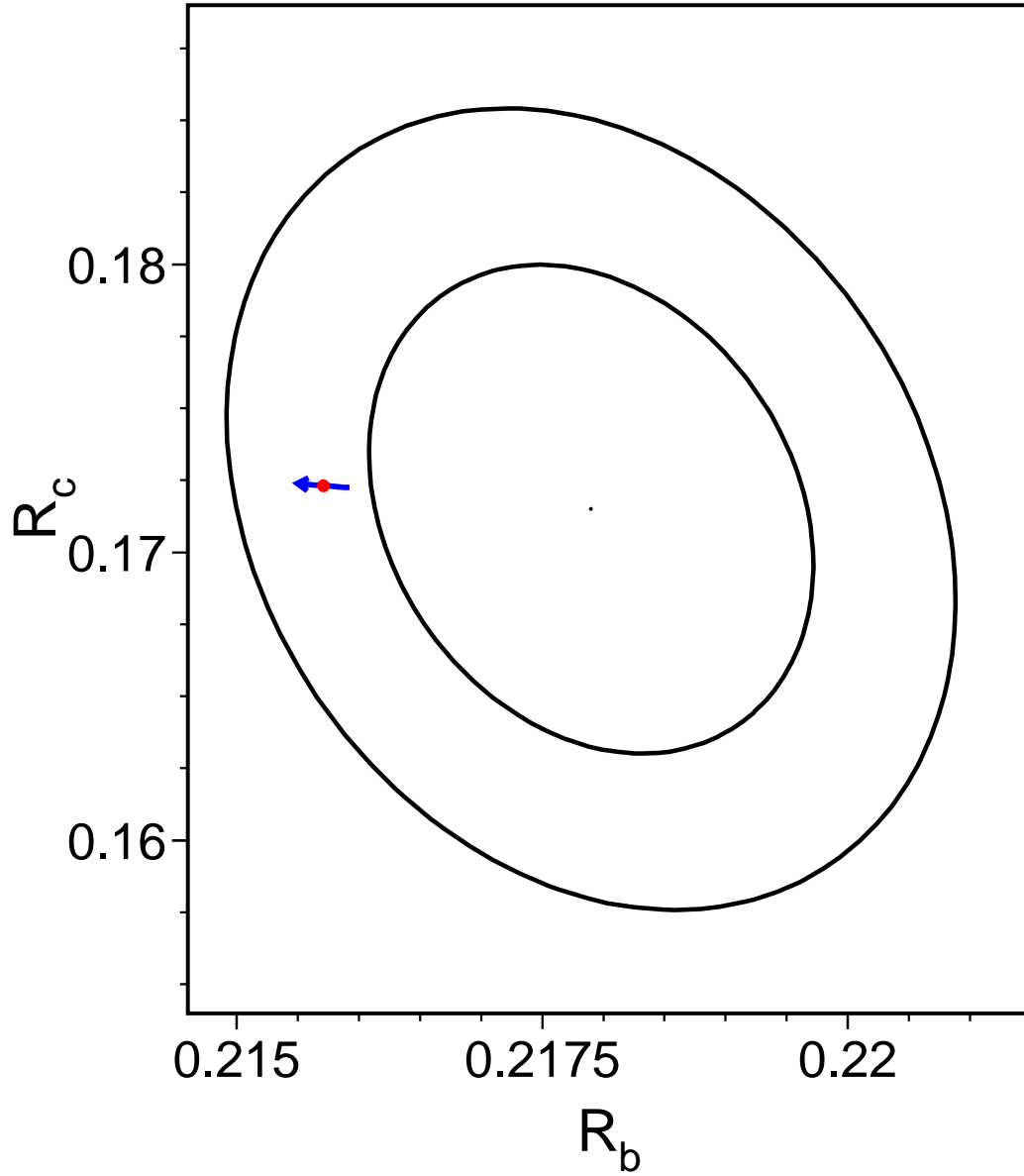


Figure 3: Contours in the R_b - R_c plane derived from LEP data, corresponding to 68% and 95% confidence levels assuming Gaussian systematic errors. The Standard Model prediction for $m_t = 175 \pm 6$ GeV is also shown. The arrow points in the direction of increasing values of m_t .

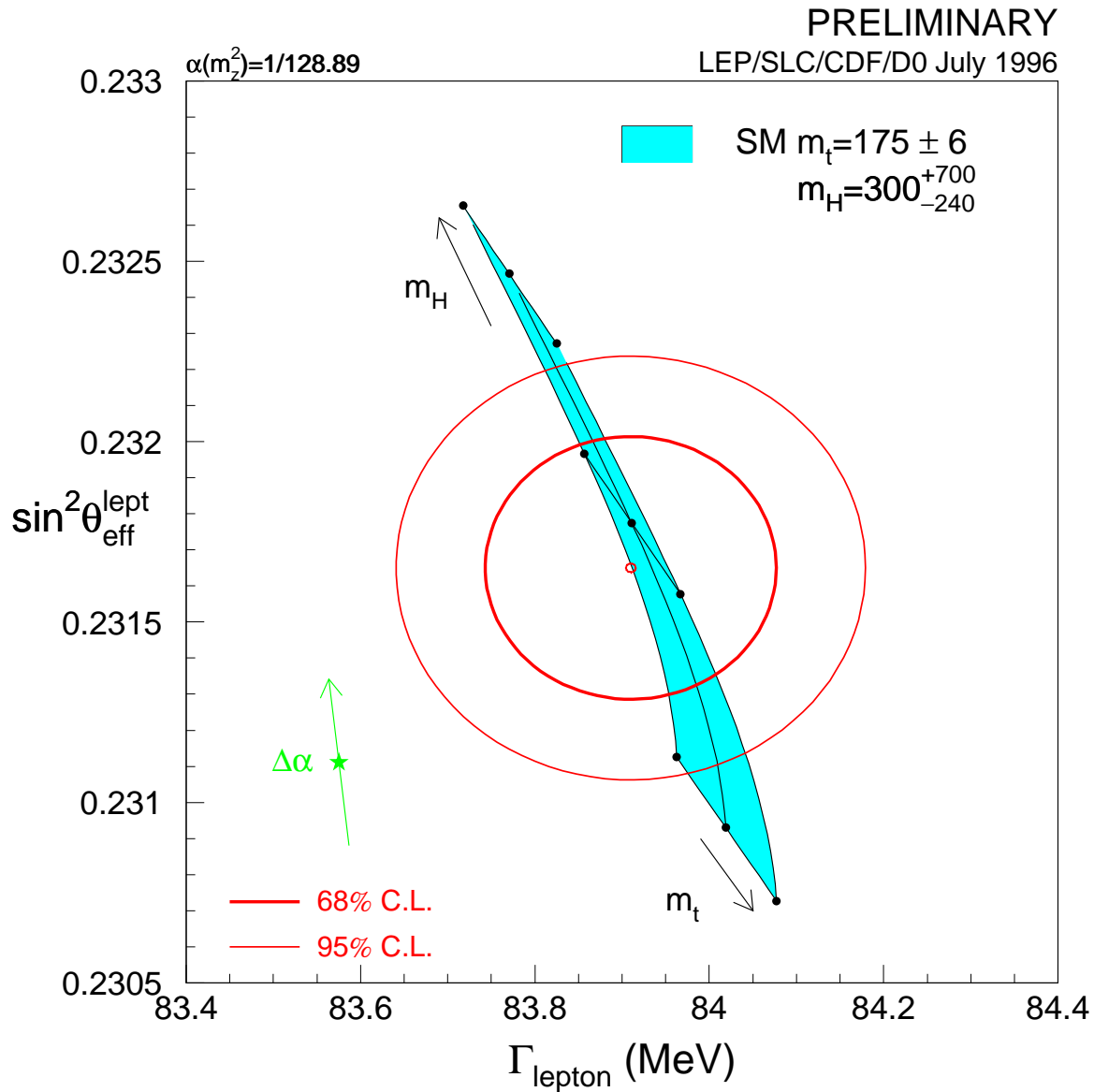


Figure 4: The LEP/SLD measurements of $\sin^2 \theta_{\text{eff}}^{\text{lept}}$ (Table 19) and $\Gamma_{\ell\ell}$ (Table 9) and the Standard Model prediction. The star shows the predictions if among the electroweak radiative corrections only the photon vacuum polarisation is included. The corresponding arrow shows variation of this prediction if $\alpha(m_Z^2)$ is changing by one standard deviation. This variation gives an additional uncertainty to the Standard Model prediction shown in the figure.

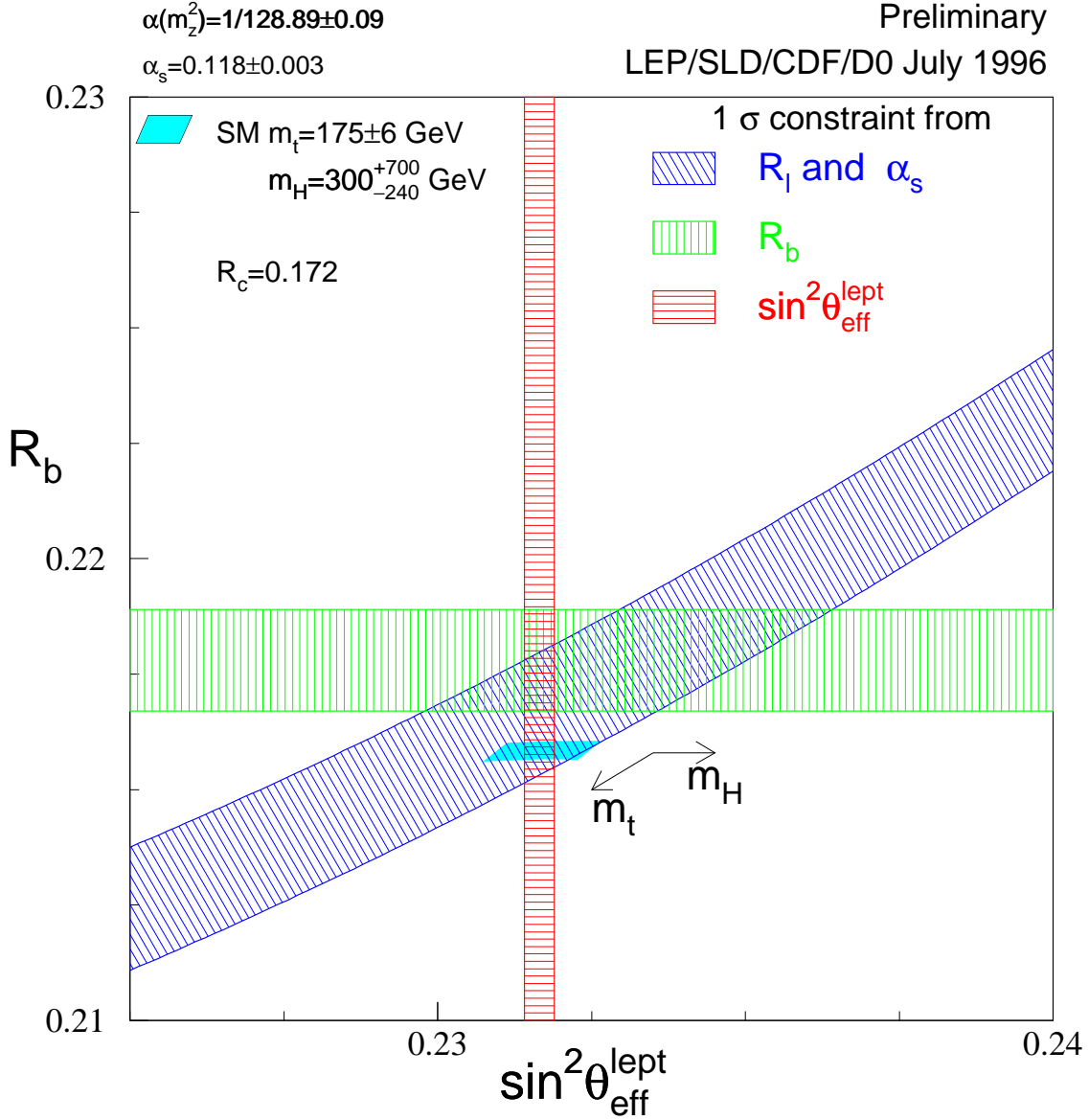


Figure 5: The LEP/SLD measurements of $\sin^2 \theta_{\text{eff}}^{\text{lept}}$ (Table 19) and R_b ($R_c = 0.172$) and the Standard Model prediction. Also shown is the constraint resulting from the measurement of R_l on these variables, assuming $\alpha_s(m_Z^2) = 0.118 \pm 0.003$, as well as the Standard Model dependence of light-quark partial widths on $\sin^2 \theta_{\text{eff}}^{\text{lept}}$. The Standard Model value for R_c is assumed.

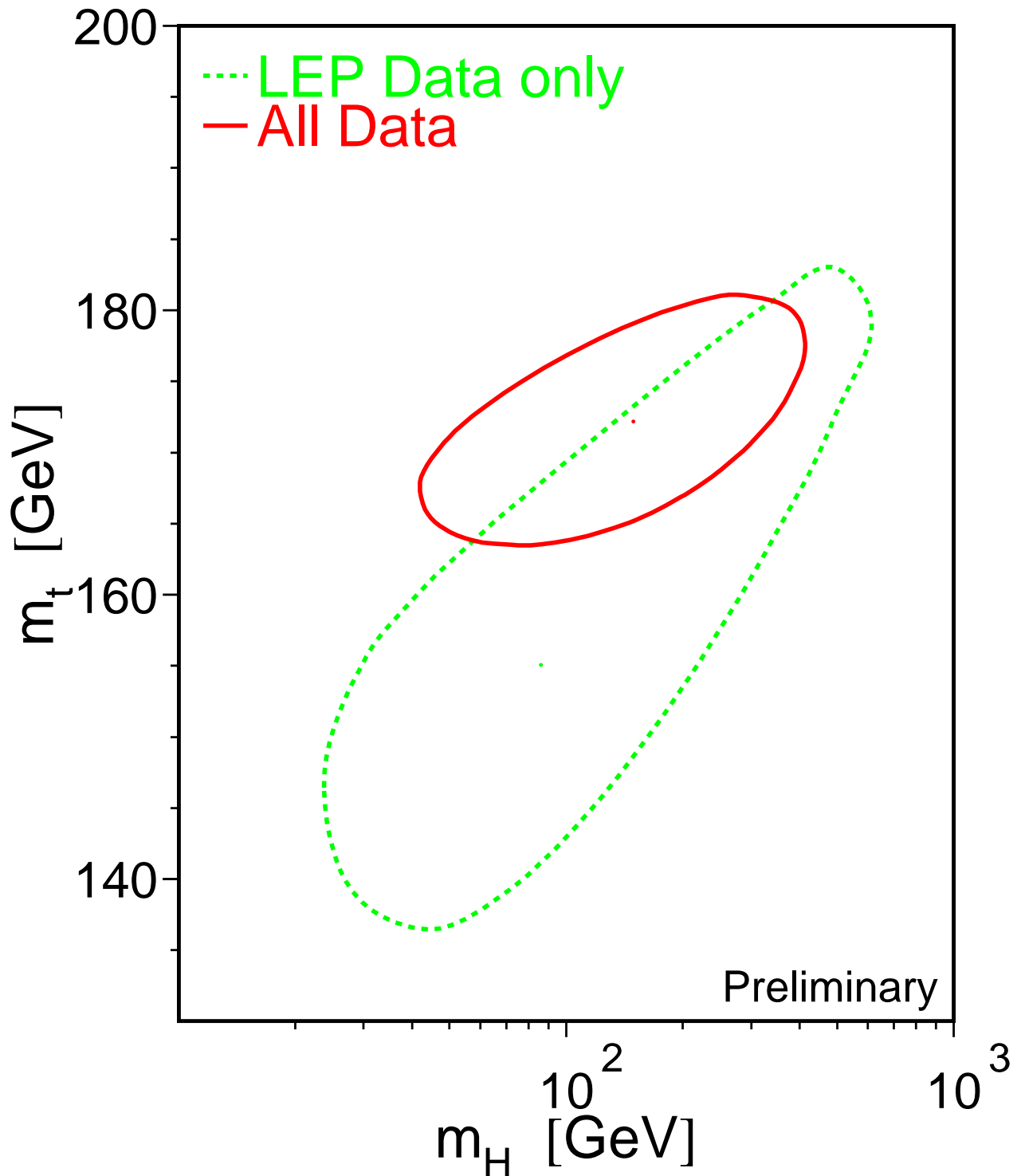


Figure 6: The 68% confidence level contours in m_t and m_H for the fits to LEP data only (dashed curve) and to all data including the CDF/DØ m_t measurement (solid curve).

Preliminary

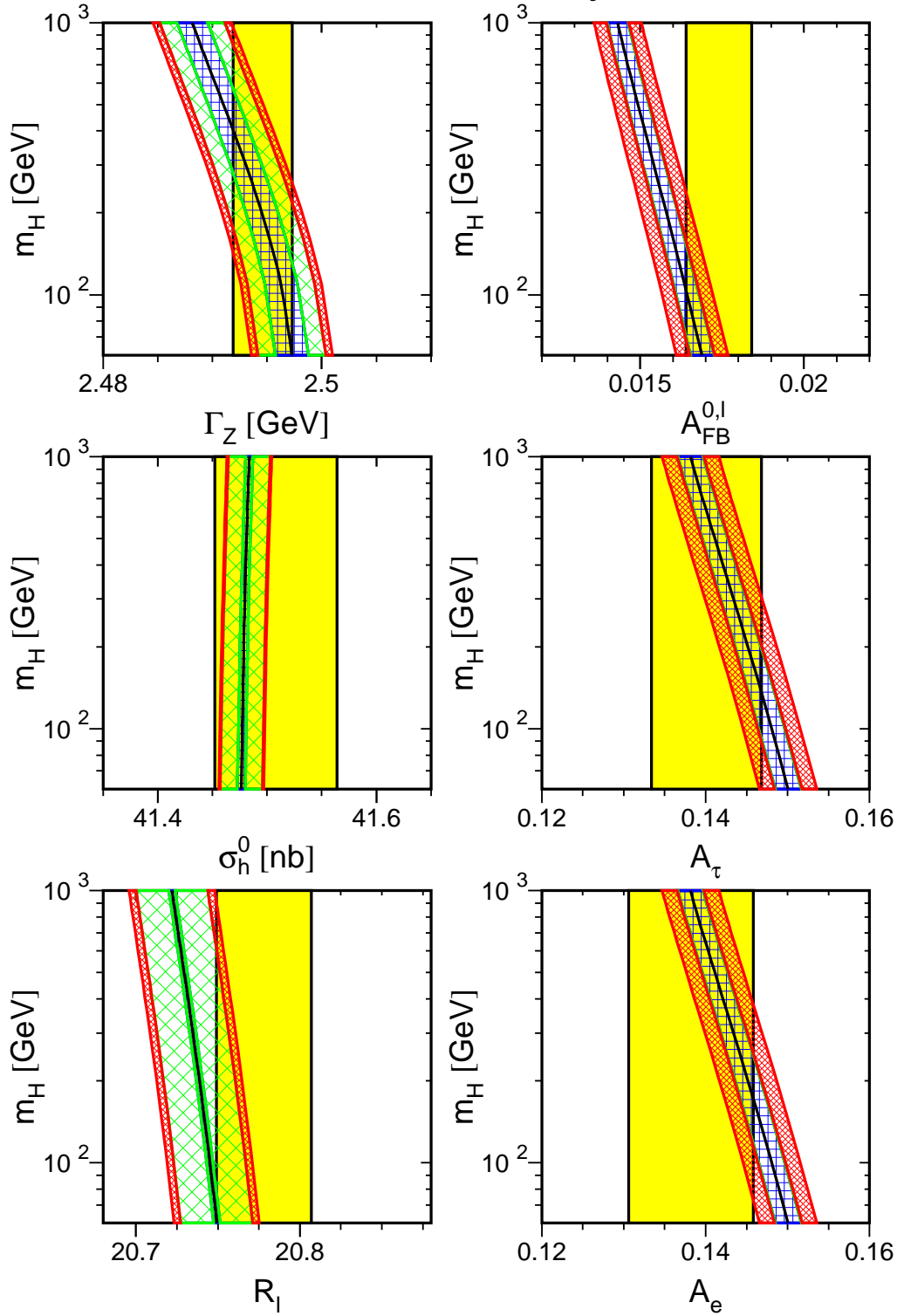


Figure 7: Comparison of LEP measurements with the Standard Model prediction as a function of m_H . The cross-hatch pattern parallel to the axes indicates the variation of the Standard Model prediction with $m_t = 175 \pm 6$ GeV, the coarse diagonal cross-hatch pattern corresponds to a variation of $\alpha_s(m_Z^2) = 0.118 \pm 0.003$, and the dense diagonal cross-hatching to the variation of $\alpha(m_Z^2)^{-1} = 128.896 \pm 0.090$. The total width of the band corresponds to the linear sum of both uncertainties. The experimental errors on the parameters are indicated as vertical bands.

Preliminary

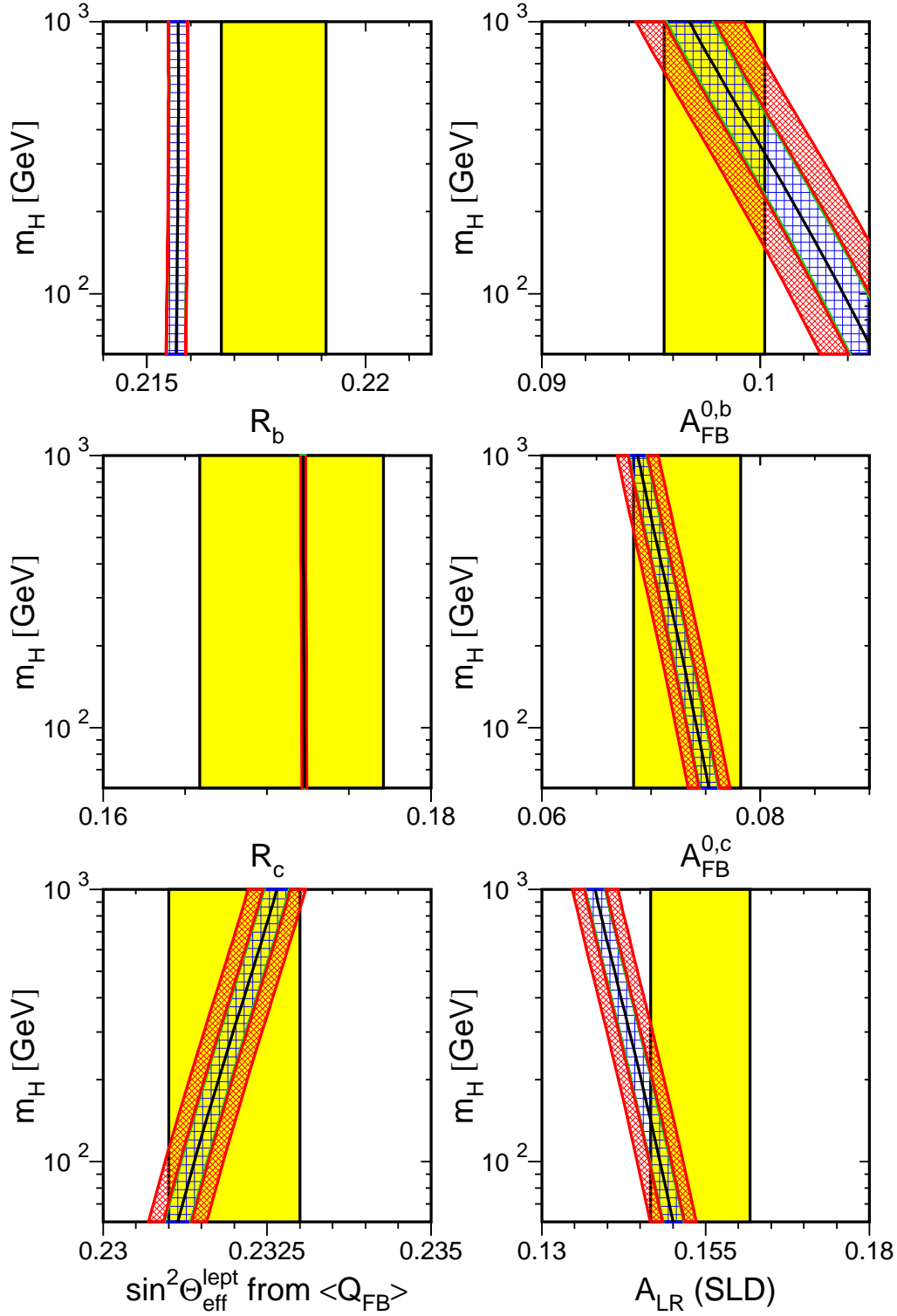


Figure 8: Comparison of LEP measurements with the Standard Model prediction as a function of m_H (*c.f.* Figure 7). For the comparison of R_b with the Standard Model the value of R_c has been fixed to its Standard Model prediction. Also shown is the comparison of the SLD measurement of A_{LR} with the Standard Model.

Preliminary

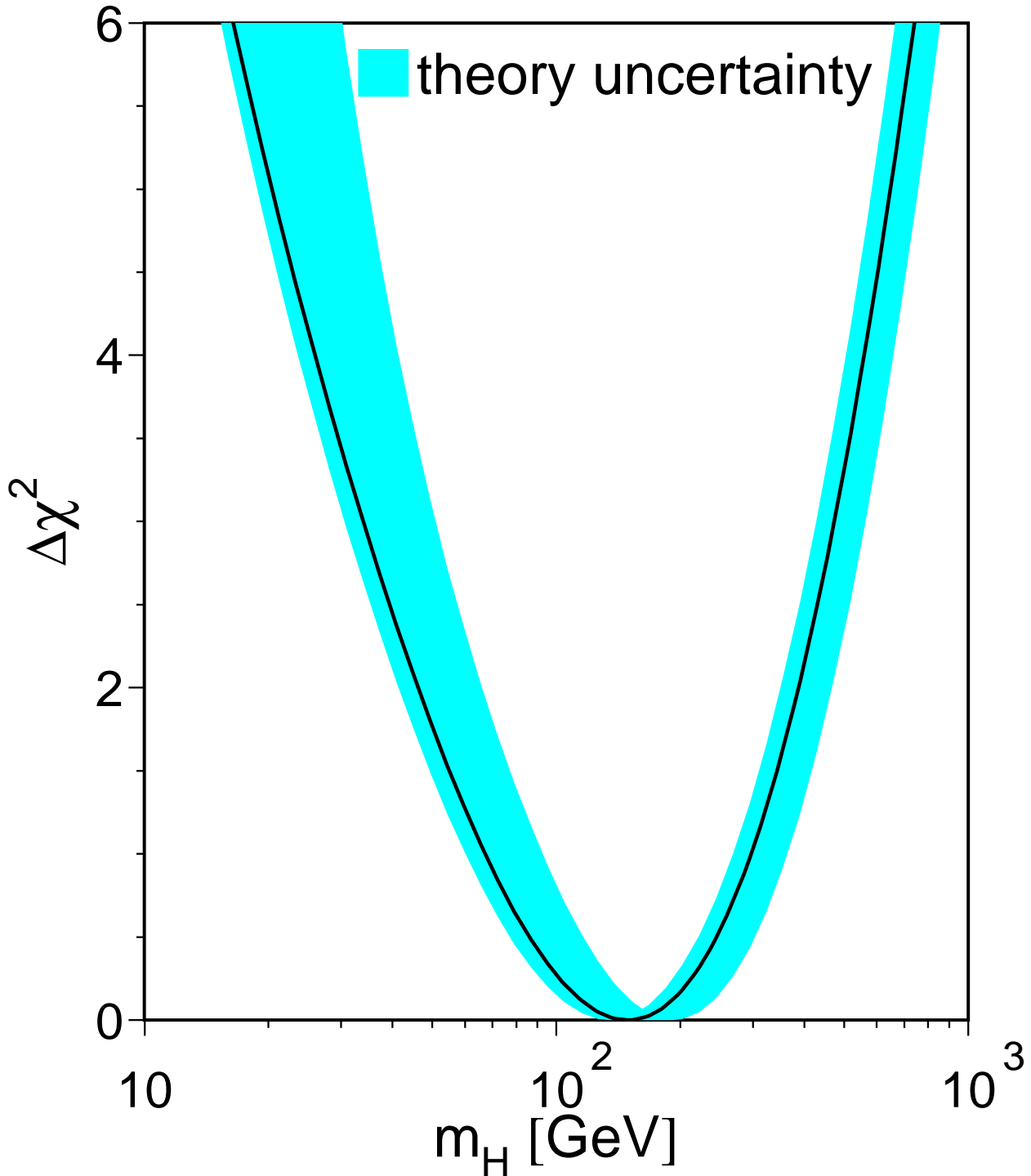


Figure 9: $\Delta\chi^2 = \chi^2 - \chi_{min}^2$ vs. m_H curve. The line is the result of the fit using all data (last column of Table 22); the band represents an estimate of the theoretical error due to missing higher order corrections.

Appendix

Heavy Flavour fit including off peak asymmetries

The full 17 parameter fit to the LEP and SLD data gave the following results:

$$\begin{aligned}R_b^0 &= 0.2178 \pm 0.0011 \\R_c^0 &= 0.1714 \pm 0.0056 \\A_{\text{FB}}^{\text{b}\bar{\text{b}}}(-2) &= 0.051 \pm 0.011 \\A_{\text{FB}}^{\text{c}\bar{\text{c}}}(-2) &= -0.038 \pm 0.019 \\A_{\text{FB}}^{\text{b}\bar{\text{b}}}(\text{pk}) &= 0.0961 \pm 0.0024 \\A_{\text{FB}}^{\text{c}\bar{\text{c}}}(\text{pk}) &= 0.0674 \pm 0.0050 \\A_{\text{FB}}^{\text{b}\bar{\text{b}}}(+2) &= 0.110 \pm 0.009 \\A_{\text{FB}}^{\text{c}\bar{\text{c}}}(+2) &= 0.138 \pm 0.016 \\\mathcal{A}_b &= 0.862 \pm 0.049 \\\mathcal{A}_c &= 0.627 \pm 0.085 \\\text{BR}(\text{b} \rightarrow \ell) &= 0.1122 \pm 0.0021 \\\text{BR}(\text{b} \rightarrow \text{c} \rightarrow \bar{\ell}) &= 0.0803 \pm 0.0034 \\\bar{\chi} &= 0.1217 \pm 0.0046 \\f(\text{D}^+) &= 0.222 \pm 0.021 \\f(\text{D}_s) &= 0.116 \pm 0.028 \\f(c_{\text{baryon}}) &= 0.082 \pm 0.022 \\P(\text{c} \rightarrow \text{D}^{*+}) \times \text{BR}(\text{D}^{*+} \rightarrow \pi^+ \text{D}^0) &= 0.1626 \pm 0.0066\end{aligned}$$

with a $\chi^2/\text{d.o.f.}$ of $49/(87 - 17)$. The corresponding correlation matrix is given in Table 23. The energy for the peak-2, peak and peak+2 results are respectively 89.55 GeV, 91.26 GeV and 92.94 GeV. Note that the asymmetry results shown here are not the pole asymmetries which have been shown in Section 4.3.2.

	1)	2)	3)	4)	5)	6)	7)	8)	9)	10)	11)	12)	13)	14)	15)	16)	17)
	R_b	R_c	$A_{\text{FB}}^{\text{bb}}(-2)$	$A_{\text{FB}}^{\text{cc}}(-2)$	$A_{\text{FB}}^{\text{bb}}(\text{pk})$	$A_{\text{FB}}^{\text{cc}}(\text{pk})$	$A_{\text{FB}}^{\text{bb}}(+2)$	$A_{\text{FB}}^{\text{cc}}(+2)$	\mathcal{A}_b	\mathcal{A}_c	BR (1)	BR (2)	$\bar{\chi}$	$f(D^+)$	$f(D_s)$	$f(c_{\text{bar}})$	PcDst
1)	1.00	-0.23	0.00	-0.01	0.00	0.01	-0.01	0.00	-0.03	0.01	-0.13	-0.02	-0.01	-0.14	-0.11	0.13	0.16
2)	-0.23	1.00	0.00	0.01	0.04	-0.06	0.01	-0.04	0.05	-0.07	0.06	0.12	0.00	-0.09	0.14	0.12	-0.60
3)	0.00	0.00	1.00	0.13	0.03	0.01	0.01	0.00	0.01	0.01	0.03	-0.03	0.09	0.00	0.00	0.00	0.00
4)	-0.01	0.01	0.13	1.00	0.02	0.02	0.01	0.00	0.00	0.00	0.01	-0.02	0.01	0.00	0.00	0.00	0.00
5)	0.00	0.04	0.03	0.02	1.00	0.10	0.07	-0.01	0.04	0.02	0.03	-0.14	0.24	0.00	0.00	0.00	-0.03
6)	0.01	-0.06	0.01	0.02	0.10	1.00	0.00	0.14	0.01	0.10	0.12	-0.21	0.12	0.00	-0.01	0.00	0.05
7)	-0.01	0.01	0.01	0.01	0.07	0.00	1.00	0.13	0.02	0.00	0.00	-0.04	0.11	0.00	0.00	0.00	0.00
8)	0.00	-0.04	0.00	0.00	-0.01	0.14	0.13	1.00	0.01	0.05	0.05	-0.08	0.04	-0.01	-0.01	0.01	0.02
9)	-0.03	0.05	0.01	0.00	0.04	0.01	0.02	0.01	1.00	0.12	0.02	-0.05	0.11	-0.01	0.01	0.01	-0.04
10)	0.01	-0.07	0.01	0.00	0.02	0.10	0.00	0.05	0.12	1.00	0.08	-0.23	0.11	0.00	-0.01	-0.01	0.04
11)	-0.13	0.06	0.03	0.01	0.03	0.12	0.00	0.05	0.02	0.08	1.00	-0.16	0.30	0.01	0.02	-0.01	-0.04
12)	-0.02	0.12	-0.03	-0.02	-0.14	-0.21	-0.04	-0.08	-0.05	-0.23	-0.16	1.00	-0.34	0.00	0.02	0.00	-0.07
13)	-0.01	0.00	0.09	0.01	0.24	0.12	0.11	0.04	0.11	0.11	0.30	-0.34	1.00	0.00	0.00	-0.01	0.00
14)	-0.14	-0.09	0.00	0.00	0.00	0.00	0.00	-0.01	-0.01	0.00	0.01	0.00	0.00	1.00	-0.30	-0.19	0.07
15)	-0.11	0.14	0.00	0.00	0.00	-0.01	0.00	-0.01	0.01	-0.01	0.02	0.02	0.00	-0.30	1.00	-0.26	-0.07
16)	0.13	0.12	0.00	0.00	0.00	0.00	0.00	0.01	0.01	-0.01	-0.01	0.00	-0.01	-0.19	-0.26	1.00	-0.05
17)	0.16	-0.60	0.00	0.00	-0.03	0.05	0.00	0.02	-0.04	0.04	-0.04	-0.07	0.00	0.07	-0.07	-0.05	1.00

Table 23: The correlation matrix for the set of the 17 heavy flavour parameters. BR(1) and BR(2) denote $\text{BR}(b \rightarrow \ell)$ and $\text{BR}(b \rightarrow c \rightarrow \bar{\ell})$ respectively, PcDst denotes $P(c \rightarrow D^{*+}) \times \text{BR}(D^{*+} \rightarrow \pi^+ D^0)$.

The Measurements used in the Heavy Flavour Averages

In the following tables, preliminary results are indicated by the symbol “†.” The values of centre-of-mass energy are given where relevant. In each table, the result used as input to the average procedure is given followed by the statistical error, the correlated and uncorrelated systematic errors, the total systematic error, and any dependence on other electroweak parameters. In the case of the asymmetries, the QCD corrected result moved to a common energy (89.55 GeV, 91.26 GeV and 92.94 GeV, respectively, for peak−2, peak and peak+2 results) is quoted as *corrected* asymmetry. The asymmetries quoted with a “‡” are not QCD corrected.

Contributions to the correlated systematic error quoted here are from any sources of error shared with one or more other results from different experiments in the same table, and the uncorrelated errors from the remaining sources. In the case of \mathcal{A}_c and \mathcal{A}_b from SLD the quoted correlated systematic error has contributions from any source shared with one or more other measurements from LEP experiment. Constants such as $a(x)$ denote the dependence on the assumed value of x^{used} , which is also given.

	ALEPH		DELPHI		L3			OPAL		SLD
	92-95† multiple [30]	90-91 lepton [23]	90-94† multiple [31]	91-92 lepton [25]	94† lifetime [32]	91 shape [29]	90-91† lepton [27]	92-94† multiple [33]	90-91 lepton [28]	93-95† lifetime [21]
R_b	0.2158	0.2162	0.2202	0.2146	0.2185	0.2220	0.2193	0.2190	0.2240	0.2149
Statistical	0.0009	0.0062	0.0014	0.0089	0.0028	0.0030	0.0081	0.0014	0.0110	0.0032
Uncorrelated	0.0008	0.0040	0.0011	0.0063	0.0027	0.0053	0.0047	0.0012	0.0045	0.0018
Correlated	0.0008	0.0031	0.0013	0.0020	0.0018	0.0036	0.0021	0.0016	0.0045	0.0011
Total Systematic	0.0011	0.0050	0.0017	0.0066	0.0032	0.0064	0.0051	0.0020	0.0063	0.0021
$a(R_c)$	-0.0033		-0.0172		-0.0251	-0.0209	-0.0232	-0.0184	-0.0132	-0.0093
R_c^{used}	0.1710		0.1720		0.1710	0.1710	0.1710	0.1710	0.1710	0.1710
$a(\text{BR}(b \rightarrow \ell))$						-0.0210				
$\text{BR}(b \rightarrow \ell)^{\text{used}} [\%]$						10.50				
$a(\text{BR}(b \rightarrow c \rightarrow \ell))$							0.0342			
$\text{BR}(b \rightarrow c \rightarrow \bar{\ell})^{\text{used}} [\%]$							7.90			
$a(f(D^+))$	-0.0011		-0.0045		-0.0066			-0.0043		-0.0009
$f(D^+)^{\text{used}}$	0.2310		0.2330		0.2310			0.2310		0.2310
$a(f(D_s))$	-0.0002		-0.0014		0.0003			-0.0005		-0.0003
$f(D_s)^{\text{used}}$	0.1100		0.1020		0.1100			0.1100		0.1100
$a(f(c_{baryon}))$	0.0002		0.0006		0.0009			0.0010		0.0004
$f(c_{baryon})^{\text{used}}$	0.0630		0.0650		0.0630			0.0630		0.0630

Table 24: The measurements of R_b .

	ALEPH		DELPHI		OPAL		
	90-91 lepton [23]	91-95† D*± [24]	92-95† lepton [24]	91-94† c count + D*± [36]	91-92 lepton [25]	90-95† D*± [37]	90-94 c count [37]
R_c	0.167	0.172	0.165	0.169	0.164	0.182	0.167
Statistical	0.005	0.010	0.007	0.008	0.008	0.011	0.011
Uncorrelated	0.015	0.009	0.005	0.007	0.017	0.014	0.011
Correlated	0.011	0.005	0.009	0.004	0.0114	0.006	0.005
Total Systematic	0.019	0.010	0.011	0.008	0.020	0.015	0.012

Table 25: The measurements of R_c .

	ALEPH		DELPHI		L3	OPAL		
	90-95 lepton [23]	90-95 lepton [23]	91-94† lepton [26]	91-94† D*± [26]	90-93† lepton [27]	91-94 jet [35]	90-95† lepton [28]	90-95 D*± [39]
\sqrt{s} (GeV)	88.380	89.380	89.43	89.54	89.56	89.52	89.40	89.45
$A_{\text{FB}}^{\text{bb}}(-2)$ Quoted	-3.4†	5.3†	6.38	1.96†	7.02†	6.30	3.48†	-8.6†
$A_{\text{FB}}^{\text{bb}}(-2)$ Corrected	5.12	5.12	6.67	2.01	7.11	6.37	3.68	-8.6
Statistical	1.88	1.88	3.80	10.48	3.50	3.40	1.73	10.8
Uncorrelated	0.04	0.04	0.16	1.13	0.36	0.21	0.15	2.4
Correlated	0.06	0.06	0.11	0.11	0.14	0.03	0.06	1.5
Total Systematic	0.07	0.07	0.19	1.14	0.38	0.21	0.16	2.8
$a(R_b)$	0.0870	0.0870	-0.7233		-1.6416	-1.8000	-0.1000	
R_b^{used}	0.2192	0.2192	0.2170		0.2160	0.2160	0.2155	
$a(R_c)$	0.0333	0.0333	0.1221		0.9126	0.0100	0.1000	
R_c^{used}	0.1710	0.1710	0.1710		0.1690	0.1730	0.1720	
$a(A_{\text{FB}}^{\text{cc}}(-2))$	-0.186	-0.186			-0.2723	-0.1980		
$A_{\text{FB}}^{\text{cc}}(-2)^{\text{used}}$	-2.34	-2.34			-2.96	-2.98		
$a(\text{BR}(b \rightarrow \ell))$	-0.236	-0.236	-0.9706		-0.9282		0.3406	
$\text{BR}(b \rightarrow \ell)^{\text{used}}$ [%]	11.34	11.34	11.00		10.50		10.90	
$a(\text{BR}(b \rightarrow c \rightarrow \ell))$	-0.102	-0.102	0.1580		-0.0658		-0.5298	
$\text{BR}(b \rightarrow c \rightarrow \ell)^{\text{used}}$ [%]	7.86	7.86	7.90		7.90		8.30	
$a(\bar{\chi})$	5.12	5.12	2.0533					
$\bar{\chi}^{\text{used}}$	0.12680	0.12680	0.12100					

Table 26: The measurements of $A_{\text{FB}}^{\text{bb}}(-2)$ (in units of 10^{-2}). The corrected asymmetries are at $\sqrt{s} = 89.55$ GeV. The numbers marked with a “†” are not QCID corrected.

	ALEPH			DELPHI			L3			OPAL		
	90-95 lepton [23]	91-95† jet [34]	91-94† lepton [26]	91-94† D*± [26]	91-94† jet [26]	90-93† lepton [27]	91-94 jet [35]	90-95† lepton [28]	90-95 D*± [39]			
\sqrt{s} (GeV)	91.210	91.187	91.23	91.23	91.23	91.27	91.25	91.24	91.22			
$A_{\text{FB}}^{\text{bb}}$ (pk) Quoted	9.65†	9.27	10.76	7.13†	9.88	10.28†	9.73	8.81†	9.40†			
$A_{\text{FB}}^{\text{bb}}$ (pk) Corrected	9.96	9.41	10.82	7.30	9.94	10.42	9.75	8.99	9.59			
Statistical	0.45	0.39	0.76	2.50	0.72	1.00	0.67	0.44	2.7			
Uncorrelated	0.10	0.26	0.21	1.27	0.36	0.37	0.31	0.13	2.1			
Correlated	0.17	0.23	0.23	0.13	0.12	0.15	0.25	0.15	0.5			
Total Systematic	0.20	0.34	0.31	1.28	0.38	0.39	0.39	0.20	2.2			
$a(R_b)$	-1.4613	-0.1840	-2.8933		-0.6000	-1.6416	-10.0900	-0.7000				
R_b^{used}	0.2192	0.2178	0.2170		0.2210	0.2160	0.2160	0.2155				
$a(R_c)$	1.0260		1.2214		0.2400	0.9126	0.1100	0.6000				
R_c^{used}	0.1710		0.1710		0.1710	0.1690	0.1730	0.1720				
$a(A_{\text{FB}}^{\text{cc}}(\text{pk}))$	0.4965					0.5752	0.7156					
$A_{\text{FB}}^{\text{cc}}(\text{pk})^{\text{used}}$	6.41					6.25	6.15					
$a(\text{BR}(b \rightarrow \ell))$	-1.2960		-3.5588			-0.6468		-0.3406				
$\text{BR}(b \rightarrow \ell)^{\text{used}}$ [%]	11.34		11.00			10.50		10.90				
$a(\text{BR}(b \rightarrow c \rightarrow \ell))$	-0.1886		0.4740			-0.2831		-0.3532				
$\text{BR}(b \rightarrow c \rightarrow \bar{\ell})^{\text{used}}$ [%]	7.86		7.90			7.90		8.30				
$a(\bar{\chi})$	3.3429		3.4467									
$\bar{\chi}^{\text{used}}$	0.12680		0.12100									

Table 27: The measurements of $A_{\text{FB}}^{\text{bb}}$ (pk) (in units of 10^{-2}). The corrected asymmetries are at $\sqrt{s} = 91.26$ GeV. The numbers marked with a “†” are not QCID corrected.

	ALEPH			DELPHI		L3	OPAL		
	90-95 lepton [23]	90-95 lepton [23]	90-95 lepton [23]	91-94† lepton [26]	91-94† D*± [26]	90-93† lepton [27]	91-94 jet [35]	90-95† lepton [28]	90-95 D*± [39]
\sqrt{s} (GeV)	92.050	92.940	93.900	93.02	92.94	92.93	92.94	92.95	93.00
$A_{\text{FB}}^{\text{bb}}(+2)$ Quoted	3.8†	10.3†	8.8†	15.24	5.63†	11.02†	17.30	10.34†	-2.10†
$A_{\text{FB}}^{\text{bb}}(+2)$ Corrected		9.97		15.16	5.72	11.20	17.30	10.49	-2.14
Statistical		1.50		3.60	9.55	2.90	2.90	1.43	9.0
Uncorrelated		0.14		0.49	1.64	0.37	0.70	0.33	2.0
Correlated		0.23		0.41	0.13	0.15	0.06	0.28	1.9
Total Systematic		0.27		0.64	1.65	0.40	0.71	0.43	2.8
$a(R_b)$		-1.86		-2.8933		-1.6416	-18.3000	-0.8000	
R_b^{used}		0.2192		0.2170		0.2160	0.2160	0.2155	
$a(R_c)$		1.43		-0.9771		0.9126	0.1600	0.8000	
R_c^{used}		0.1710		0.1710		0.1690	0.1730	0.1720	
$a(A_{\text{FB}}^{\text{cc}}(+2))$		0.913				1.1156	0.6800		
$A_{\text{FB}}^{\text{cc}}(+2)^{\text{used}}$		12.51				12.13	12.00		
$a(\text{BR}(b \rightarrow c \rightarrow \ell))$		-1.65		-3.2353		-0.6300		-1.3625	
$\text{BR}(b \rightarrow \ell)^{\text{used}} [\%]$		11.34		11.00		10.50		10.90	
$a(\text{BR}(b \rightarrow c \rightarrow \bar{\ell}))$		-0.241		0.4740		-0.3028		0.7064	
$\text{BR}(b \rightarrow c \rightarrow \bar{\ell})^{\text{used}} [\%]$		7.86		7.90		7.90		8.30	
$a(\bar{\chi})$		6.409		4.7667					
$\bar{\chi}^{\text{used}}$		0.12680		0.12100					

Table 28: The measurements of $A_{\text{FB}}^{\text{bb}}(+2)$ (in units of 10^{-2}). The corrected asymmetries are at $\sqrt{s} = 92.94$ GeV. The numbers marked with a “†” are not QCID corrected.

	ALEPH	DELPHI	OPAL	
Tagging	91-94† D*± [38]	91-94† D*± [26]	90-95† lepton [28]	91-95 D*± [39]
\sqrt{s} (GeV)	89.400	89.54	89.40	89.34
$A_{\text{FB}}^{\text{cc}}(-2)$ Quoted	-4.90†	0.20†	-6.81†	3.9†
$A_{\text{FB}}^{\text{cc}}(-2)$ Corrected	-4.05	0.26	-6.52	4.30
Statistical	7.60	5.19	2.44	5.1
Uncorrelated	0.85	0.55	0.38	0.72
Correlated	0.06	0.07	0.29	0.50
Total Systematic	0.85	0.56	0.48	0.88
$a(R_b)$ R_b^{used}			-3.4000 0.2155	
$a(R_c)$ R_c^{used}			3.2000 0.1720	
$a(A_{\text{FB}}^{\text{bb}}(-2))$ $A_{\text{FB}}^{\text{bb}}(-2)^{\text{used}}$	0.2295 -1.34			
$a(\text{BR}(b \rightarrow \ell))$ $\text{BR}(b \rightarrow \ell)^{\text{used}}$ [%]			-1.7031 10.90	
$a(\text{BR}(b \rightarrow c \rightarrow \ell))$ $\text{BR}(b \rightarrow c \rightarrow \ell)^{\text{used}}$ [%]			-1.4128 8.30	

Table 29: The measurements of $A_{\text{FB}}^{\text{cc}}(-2)$ (in units of 10^{-2}). The corrected asymmetries are at $\sqrt{s} = 89.55$ GeV. The numbers marked with a “†” are not QCD corrected.

	ALEPH		DELPHI		L3	OPAL	
Tagging	90-91 lepton [23]	91-94† D*± [38]	91-94† lepton [26]	91-94† D*± [26]	90-91 lepton [27]	90-95† lepton [28]	90-95 D*± [39]
\sqrt{s} (GeV)	91.260	91.200	91.23	91.23	91.24	91.24	91.22
$A_{\text{FB}}^{\text{cc}}$ (pk) Quoted	9.10†	6.40†	8.42	7.52†	7.84†	5.82†	6.30†
$A_{\text{FB}}^{\text{cc}}$ (pk) Corrected	9.19	6.76	8.57	7.74	8.02	5.97	6.46
Statistical	2.00	1.30	1.39	1.21	3.70	0.59	1.2
Uncorrelated	1.56	0.20	0.91	0.55	2.42	0.39	0.43
Correlated	1.05	0.18	0.75	0.12	0.60	0.48	0.36
Total Systematic	1.88	0.27	1.18	0.57	2.50	0.62	0.56
$a(R_b)$ R_b^{used}			3.6167 0.2170		4.3200 0.2160	4.1000 0.2155	
$a(R_c)$ R_c^{used}			-6.3514 0.1710		-6.7600 0.1690	-3.8000 0.1720	
$a(A_{\text{FB}}^{\text{bb}})$ $A_{\text{FB}}^{\text{bb}}(\text{pk})^{\text{used}}$		-1.5110 8.81			6.4274 8.84		
$a(\text{BR}(b \rightarrow \ell))$ $\text{BR}(b \rightarrow \ell)^{\text{used}}$ [%]			4.8529 11.00		3.5007 10.50	5.1094 10.90	
$a(\text{BR}(b \rightarrow c \rightarrow \ell))$ $\text{BR}(b \rightarrow c \rightarrow \ell)^{\text{used}}$ [%]			-3.7920 7.90		-3.2917 7.90	-1.7660 8.30	

Table 30: The measurements of $A_{\text{FB}}^{\text{cc}}$ (pk) from D* meson and lepton-tag analyses (in units of 10^{-2}). The corrected asymmetries are at $\sqrt{s} = 91.26$ GeV. The numbers marked with a “†” are not QCD corrected.

	ALEPH	DELPHI	OPAL	
Tagging	91-94† D*± [38]	91-94† D*± [26]	90-95† lepton [28]	90-95 D*± [39]
\sqrt{s} (GeV)	93.000	92.94	92.95	93.00
$A_{\text{FB}}^{\text{cc}}(+2)$ Quoted	10.90‡	7.97‡	15.43‡	15.80‡
$A_{\text{FB}}^{\text{cc}}(+2)$ Corrected	10.85	8.05	15.56	15.93
Statistical	6.10	4.55	2.0	4.1
Uncorrelated	0.71	0.55	0.57	0.66
Correlated	0.28	0.17	0.79	0.84
Total Systematic	0.77	0.58	0.97	1.07
$a(R_b)$ R_b^{used}			9.6000 0.2155	
$a(R_c)$ R_c^{used}			-8.9000 0.1720	
$a(A_{\text{FB}}^{\text{bb}}(+2))$ $A_{\text{FB}}^{\text{bb}}(+2)^{\text{used}}$	-2.0639 12.04			
$a(\text{BR}(b \rightarrow \ell))$ $\text{BR}(b \rightarrow \ell)^{\text{used}}$ [%]			9.5375 10.90	
$a(\text{BR}(b \rightarrow c \rightarrow \ell))$ $\text{BR}(b \rightarrow c \rightarrow \bar{\ell})^{\text{used}}$ [%]			-1.5894 8.30	

Table 31: The measurements of $A_{\text{FB}}^{\text{cc}}(+2)$ (in units of 10^{-2}). The corrected asymmetries are at $\sqrt{s} = 92.94$ GeV. The numbers marked with a “‡” are not QCD corrected.

	SLD		
Tagging	93-95† lepton [22]	93-95† jet [22]	94-95† K± [22]
\sqrt{s} (GeV)	91.28	91.28	91.28
\mathcal{A}_b	0.882	0.843	0.907
Statistical	0.068	0.046	0.094
Uncorrelated	0.037	0.049	0.092
Correlated	0.021	0.000	0.007
Total Systematic	0.043	0.049	0.092
$a(R_b)$ R_b^{used}	-0.4302 0.2216	-0.1308 0.2180	-0.0218 0.2180
$a(R_c)$ R_c^{used}	0.0800 0.1600	0.1328 0.1710	0.0030 0.1710
$a(\mathcal{A}_c)$ $\mathcal{A}_c^{\text{used}}$		0.0809 0.666	-0.1332 0.666
$a(\text{BR}(b \rightarrow \ell))$ $\text{BR}(b \rightarrow \ell)^{\text{used}}$ [%]	-0.3038 10.75		
$a(\text{BR}(b \rightarrow c \rightarrow \ell))$ $\text{BR}(b \rightarrow c \rightarrow \bar{\ell})^{\text{used}}$ [%]	0.1095 8.10		
$a(\bar{\chi})$ $\bar{\chi}^{\text{used}}$	0.4197 0.12200		0.2229 0.13000

Table 32: The measurements of \mathcal{A}_b .

Tagging	SLD	
	93-95† lepton [22]	93-95† D*± [22]
\sqrt{s} (GeV)	91.28	91.28
\mathcal{A}_c	0.612	0.640
Statistical	0.102	0.110
Uncorrelated	0.042	0.053
Correlated	0.050	0.020
Total Systematic	0.065	0.057
$a(R_b)$	0.1173	
R_b^{used}	0.2216	
$a(R_c)$	-0.4864	
R_c^{used}	0.1600	
$a(\mathcal{A}_b)$		-0.1278
$\mathcal{A}_b^{\text{used}}$		0.935
$a(\text{BR}(b \rightarrow \ell))$	0.4580	
$\text{BR}(b \rightarrow \ell)^{\text{used}}$ [%]	10.75	
$a(\text{BR}(b \rightarrow c \rightarrow \ell))$	-0.4991	
$\text{BR}(b \rightarrow c \rightarrow \bar{\ell})^{\text{used}}$ [%]	8.10	

Table 33: The measurements of \mathcal{A}_c .

Tagging	ALEPH		DELPHI	L3	OPAL
	90-91 lepton [23]	92-93† multiple [23]	91-92 lepton [25]	90-91† lepton [27]	90-91 lepton [28]
$\text{BR}(b \rightarrow \ell)$	11.20	11.01	11.30	11.42	10.60
Statistical	0.33	0.10	0.45	0.48	0.60
Uncorrelated	0.32	0.20	0.50	0.30	0.39
Correlated	0.27	0.21	0.46	0.21	0.53
Total Systematic	0.42	0.29	0.68	0.37	0.66
$a(R_c)$				0.6107	0.2236
R_c^{used}				0.1710	0.1710
$a(\text{BR}(b \rightarrow c \rightarrow \ell))$				0.4608	
$\text{BR}(b \rightarrow c \rightarrow \bar{\ell})^{\text{used}}$ [%]				7.90	
$a(\bar{\chi})$		0.2075			
$\bar{\chi}^{\text{used}}$		0.12610			

Table 34: The measurements of $\text{BR}(b \rightarrow \ell)$ from the lepton-tag analyses.

Tagging	ALEPH		DELPHI	OPAL
	90-91 lepton [23]	92-93† multiple [23]	91-92 lepton [25]	90-91 lepton [28]
BR($b \rightarrow c \rightarrow \ell$)	8.81	7.68	7.90	8.40
Statistical	0.25	0.18	0.49	0.40
Uncorrelated	0.40	0.25	0.95	0.57
Correlated	0.69	0.42	0.78	0.38
Total Systematic	0.80	0.49	1.23	0.68
$a(R_c)$				0.3157
R_c^{used}				0.1710
$a(\bar{\chi})$		-0.5108		
$\bar{\chi}^{\text{used}}$		0.12610		

Table 35: The measurements of BR($b \rightarrow c \rightarrow \bar{\ell}$) from the lepton-tag analyses.

Tagging	ALEPH	DELPHI	L3	OPAL
	90-95† lepton [23]	91-92 lepton [25]	90-93† lepton [27]	90-95† lepton [28]
$\bar{\chi}$	0.12461	0.14900	0.12530	0.11390
Statistical	0.00515	0.02000	0.01100	0.00540
Uncorrelated	0.00244	0.01044	0.00516	0.00306
Correlated	0.00403	0.01192	0.00266	0.00324
Total Systematic	0.00471	0.01584	0.00581	0.00446
$a(R_b)$	0.0341		0.0009	
R_b^{used}	0.2192		0.2160	
$a(R_c)$	0.0009		0.0007	
R_c^{used}	0.1710		0.1690	
$a(\text{BR}(b \rightarrow \ell))$	0.0524		0.0462	0.0170
$\text{BR}(b \rightarrow \ell)^{\text{used}} [\%]$	11.34		10.50	10.90
$a(\text{BR}(b \rightarrow c \rightarrow \ell))$	-0.0440		-0.0342	-0.0318
$\text{BR}(b \rightarrow c \rightarrow \bar{\ell})^{\text{used}} [\%]$	7.86		7.90	8.30

Table 36: The measurements of $\bar{\chi}$ from the lepton-tag analyses.

Tagging	DELPHI	OPAL
	91-94† $D^{*\pm}$ [36]	90-94† $D^{*\pm}$ [37]
$P(c \rightarrow D^{*+}) \times \text{BR}(D^{*+} \rightarrow \pi^+ D^0)$	0.1678	0.1510
Statistical	0.0069	0.0110
Uncorrelated	0.0065	0.0108
Correlated	0.0011	0.0020
Total Systematic	0.0066	0.0110

Table 37: The measurements of $P(c \rightarrow D^{*+}) \times \text{BR}(D^{*+} \rightarrow \pi^+ D^0)$.

References

- [1] The LEP Collaborations ALEPH, DELPHI, L3, OPAL and the LEP Electroweak Working Group, *A Combination of Preliminary LEP Electroweak Measurements and Constraints on the Standard Model*, CERN-PPE/95-172.
- [2] LEP Electroweak Working Group, *An Investigation of the Interference between Photon and Z-Boson Exchange*, Internal Note, LEPEWWG/LS/96-02, ALEPH 96-108 PHYSIC 96-99, DELPHI 96-120 PHYS 630, L3 Note 1976, OPAL Technical Note TN 400, 12 August 1996.
- [3] The LEP Collaborations ALEPH, DELPHI, L3, OPAL and the LEP Electroweak Working Group, *Combined Preliminary Data on Z Parameters from the LEP Experiments and Constraints on the Standard Model*, CERN-PPE/94-187.
- [4] The LEP Experiments: Aleph, Delphi, L3 and Opal, Nucl. Inst. Meth. **A378** (1996) 101.
- [5] ALEPH Collaboration, D. Decamp *et al.*, Z. Phys. **C48** (1990) 365;
ALEPH Collaboration, D. Decamp *et al.*, Z. Phys. **C53** (1992) 1;
ALEPH Collaboration, D. Buskulic *et al.*, Z. Phys. **C60** (1993) 71;
ALEPH Collaboration, D. Buskulic *et al.*, Z. Phys. **C62** (1994) 539;
ALEPH Collaboration, *Preliminary Results on Z Production Cross Section and Lepton Forward-Backward Asymmetries using the 1990-1995 Data*, contributed paper to ICHEP96, Warsaw, 25-31 July 1996, **PA-07-069**.
- [6] DELPHI Collaboration, P. Aarnio *et al.*, Nucl. Phys. **B367** (1991) 511;
DELPHI Collaboration, P. Abreu *et al.*, Nucl. Phys. **B417** (1994) 3;
DELPHI Collaboration, P. Abreu *et al.*, Nucl. Phys. **B418** (1994) 403;
DELPHI Collaboration, DELPHI Note 95-62 PHYS 497, July 1995;
DELPHI Collaboration, DELPHI Note 96-118 CONF 65, contributed paper to ICHEP96, Warsaw, 25-31 July 1996, **PA-07-001**.
- [7] L3 Collaboration, B. Adeva *et al.*, Z. Phys. **C51** (1991) 179;
L3 Collaboration, O. Adriani *et al.*, Phys. Rep. **236** (1993) 1;
L3 Collaboration, M. Acciarri *et al.*, Z. Phys. **C62** (1994) 551;
L3 Collaboration, *Preliminary L3 Results on Electroweak Parameters using 1990-95 Data*, L3 Note 1980, August 1996, available via <http://hpl3sn02.cern.ch/note/note-1980.ps.gz>.
- [8] OPAL Collaboration, G. Alexander *et al.*, Z. Phys. **C52** (1991) 175;
OPAL Collaboration, P.D. Acton *et al.*, Z. Phys. **C58** (1993) 219;
OPAL Collaboration, R. Akers *et al.*, Z. Phys. **C61** (1994) 19;
OPAL Collaboration, *A Preliminary Update of the Z Line Shape and Lepton Asymmetry Measurements with the 1993 and 1994 Data*, OPAL Physics Note PN166, February 1995;
OPAL Collaboration, *The Preliminary OPAL SiW luminosity analysis: Results for the 1994 Summer conferences*, OPAL Physics Note PN142, July 1994;
OPAL Collaboration, *A Preliminary Update of the Z Line Shape and Lepton Asymmetry Measurements with a Revised 1993-1994 LEP Energy and 1995 Lepton Asymmetry*, OPAL Physics Note PN242, July 1996;
OPAL Collaboration, *Measurements of Lepton Pair Asymmetries using the 1995 Data*, contributed paper to ICHEP96, Warsaw, 25-31 July 1996 **PA07-015**.
- [9] A. Arbuzov, *et al.*, Phys. Lett. **B383** (1996) 238;
S. Jadach, *et al.*, "Update of the Monte Carlo program BHLUMI for Bhabha scattering at low angles to version 4.04", CERN-TH/96-156, UTHEP-96-0601, June 1996, submitted to

- [10] S. Jadach, E. Richter-Waś, B.F.L. Ward and Z. Waś, *Phys. Lett.* **B353** (1995) 362.
- [11] LEP Energy Working Group, R. Assmann et al., *Z. Phys.* **C66** (1995) 567.
- [12] G. Wilkinson, *The determination of the LEP energy in the 1995 Z^0 scan*, talk presented at ICHEP96, Warsaw, 25-31 July 1996, to appear in the proceedings.
- [13] The LEP Collaborations ALEPH, DELPHI, L3, OPAL and the LEP Electroweak Working Group, *Updated Parameters of the Z Resonance from Combined Preliminary Data of the LEP Experiments*, CERN-PPE/93-157.
- [14] See, for example, M. Consoli *et al.*, in “Z Physics at LEP 1”, CERN Report CERN 89-08 (1989), eds G. Altarelli, R. Kleiss and C. Verzegnassi, Vol. 1, p. 7.
- [15] LEP Energy Working Group note 96-07, E. Lancon and A. Blondel, *Determination of the LEP Energy Spread Using Experimental Constraints*.
- [16] ALEPH Collaboration, D. Buskulic *et al.*, *Zeit. Phys.* **C69** (1996) 183.
- [17] DELPHI Collaboration, P. Abreu *et al.*, *Z. Phys.* **C67** (1995) 183;
DELPHI Collaboration, *An updated measurement of tau polarisation*, DELPHI 96-114 CONF 42, contributed paper to ICHEP96, Warsaw, 25-31 July 1996, **PA07-008**.
- [18] L3 Collaboration, O. Acciari *et al.*, *Phys. Lett.* **B341** (1994) 245;
L3 Collaboration, *A Preliminary Update of A_τ and A_e Using 1994 Data*, contributed paper ICHEP96, Warsaw, 25-31 July 1996, **PA07-56**.
The 1994 data have been combined with the earlier data using a 100% correlation of the systematic errors.
- [19] OPAL Collaboration, G. Alexander *et al.*, *A Precise Measurement of the Tau Polarization and its Forward-Backward Asymmetry at LEP* CERN-PPE/96-078, submitted to *Z. Phys. C*.
- [20] The LEP heavy flavour group, *Presentation of LEP Electroweak Heavy Flavour Results for Summer 1996 Conferences*, LEPHF/96-01, ALEPH Note 96-099, DELPHI 96-67 PHYS 627, L3 Note 1969, OPAL Technical Note TN391.
- [21] SLD Collaboration, G. Crawford, talk presented at ICHEP96, Warsaw, 25-31 July 1996.
- [22] SLD Collaboration, D. Falciari, talk presented at ICHEP96, Warsaw, 25-31 July 1996.
- [23] ALEPH Collaboration, D. Buskulic *et al.*, *Z. Phys.* **C62** (1994) 179;
ALEPH Collaboration, D. Buskulic *et al.*, *Phys. Lett.* **B384** (1996) 414;
ALEPH Collaboration, D. Buskulic *et al.*, *Measurement of the semileptonic b branching ratios from inclusive leptons in Z decays*, Contributed Paper to EPS-HEP-95 Brussels, **eps0404**.
This note may be found at <http://alephwww.cern.ch/ALPUB/oldconf/HEP95/HEP95.html>.
- [24] ALEPH Collaboration, *Measurement of the partial decay width of the Z into $c\bar{c}$ quarks* contributed paper to ICHEP96, Warsaw, 25-31 July 1996 **PA10-016**. The results of the exclusive-exclusive and inclusive-exclusive double-tag D-meson measurements have been averaged for this note.
- [25] DELPHI Collaboration, P. Abreu *et al.*, *Z. Phys.* **C66** (1995) 323.

- [26] DELPHI Collaboration, P. Abreu *et al.*, Z. Phys **C65** (1995) 569;
 DELPHI Collaboration, P. Abreu *et al.*, Z. Phys **C66** (1995) 341;
 DELPHI Collaboration, *Measurement of the Forward-Backward Asymmetries of $e^+e^- \rightarrow Z \rightarrow b\bar{b}$ and $e^+e^- \rightarrow Z \rightarrow c\bar{c}$* , DELPHI 95-87 PHYS 522.
 This and all other Delphi notes are available at <http://wwwcn.cern.ch/~pubxx/www/delsec/delnote/>.
- [27] L3 Collaboration, O. Adriani *et al.*, Phys. Lett. **B292** (1992) 454;
 L3 Collaboration, M. Acciarri *et al.*, Phys. Lett. **B335** (1994) 542;
 L3 Collaboration, *Measurement of R_b and $BR(b \rightarrow \ell X)$ from b -quark semileptonic decays*, L3 Note 1449, July 16 1993;
 L3 Collaboration, *L3 Results on $A_{FB}^{b\bar{b}}$, $A_{FB}^{c\bar{c}}$ and χ for the Glasgow Conference*, L3 Note 1624;
 L3 Collaboration, *L3 Results on R_b and $BR(b \rightarrow \ell)$ for the Glasgow Conference*, L3 Note 1625.
- [28] OPAL Collaboration, G. Alexander *et al.*, Z. Phys. **C70** (1996) 357;
 OPAL Collaboration, R. Akers *et al.*, *Updated Measurement of the Heavy Quark Forward-Backward Asymmetries and Average B Mixing Using Leptons in Multihadronic Events*, OPAL Physics Note PN226 contributed paper to ICHEP96, Warsaw, 25-31 July 1996 **PA05-007**.
- [29] L3 Collaboration, O. Adriani *et al.*, Phys. Lett. **B307** (1993) 237.
- [30] ALEPH Collaboration, *Measurement of R_b using a Lifetime-Mass Tag*, contributed paper to ICHEP96, Warsaw, 25-31 July 1996 **PA10-014**;
 ALEPH Collaboration, *A Measurement of R_b using Mutually Exclusive Tags*, contributed paper to ICHEP96, Warsaw, 25-31 July 1996 **PA10-015**.
- [31] DELPHI Collaboration, P. Abreu *et al.*, Z. Phys. **C70** (1996) 531;
 DELPHI Collaboration, P. Abreu *et al.*, *Measurement of the partial decay width $R_b = \Gamma_{b\bar{b}}/\Gamma_{had}$ with the DELPHI detector at LEP*, contributed paper to ICHEP96, Warsaw, 25-31 July 1996 **PA01-061**.
- [32] L3 Collaboration, *Measurement of the Z Branching Fraction into Bottom Quarks Using Lifetime Tags*, contributed paper to ICHEP96, Warsaw, 25-31 July 1996 **PA05-049**.
- [33] OPAL Collaboration, R. Akers *et al.*, Z. Phys. **C65** (1995) 17;
 OPAL Collaboration, *An Update of the Measurement of $\Gamma_{b\bar{b}}/\Gamma_{had}$ using a Double Tagging Method*, OPAL Physics Note PN181.
- [34] ALEPH Collaboration, D. Buskulic *et al.*, Phys. Lett. **B335** (1994) 99;
 ALEPH Collaboration, *An Upgraded Measurement of $A_{FB}^{b\bar{b}}$ from the charge asymmetry in Lifetime Tagged Z Decays* contributed paper to ICHEP96, Warsaw, 25-31 July 1996 **PA10-018**.
- [35] OPAL Collaboration, R. Akers *et al.*, Z. Phys. **C67** (1995) 365.
- [36] DELPHI Collaboration, *Summary of R_c measurements in DELPHI*, DELPHI 96-110 CONF 37 contributed paper to ICHEP96, Warsaw, 25-31 July 1996 **PA01-060**.
- [37] OPAL Collaboration, R. Akers *et al.*, Z. Phys. **C67** (1995) 27;
 OPAL Collaboration, G. Alexander *et al.*, Z. Phys. **C72** (1996) 1;
 OPAL Collaboration, *A measurement of $BR(c \rightarrow D^*)$ and $\Gamma_{c\bar{c}}/\Gamma_{had}$ using a double tagging method*, OPAL Physics Note PN227 contributed paper to ICHEP96, Warsaw, 25-31 July 1996 **PA05-011**.
- [38] ALEPH Collaboration, D. Buskulic *et al.*, Z. Phys. **C62** (1994) 1;
 ALEPH Collaboration, D. Buskulic *et al.*, *The Forward-Backward Asymmetry for Charm Quarks at the Z pole: an Update*, Contributed Paper to EPS-HEP-95 Brussels, **eps0634**.
 This note may be found at <http://alephwww.cern.ch/ALPUB/oldconf/HEP95/HEP95.html>.

- [39] OPAL Collaboration, CERN-PPE/96-101 24 July 1996.
- [40] D. Bardin *et al.*, Z. Phys. **C44** (1989) 493; Comp. Phys. Comm. **59** (1990) 303; Nucl. Phys. **B351**(1991) 1; Phys. Lett. **B255** (1991) 290 and CERN-TH 6443/92 (May 1992).
- [41] A. Djouadi, B. Lampe and P.M. Zerwas, Z. Phys. **C67** (1995) 123.
- [42] G. Altarelli and B. Lampe, Nucl. Phys. **B391** (1993) 3.
- [43] CLEO Collaboration, M. Artuso *et al.*, *Measurement of the branching fraction for $D_s^- \rightarrow \phi\pi^-$* , CLNS 95/1387, CLEO 95-23.
- [44] ALEPH Collaboration, *Measurement of the branching fraction for $D^0 \rightarrow K^- \pi^+$* , contributed paper to ICHEP96, Warsaw, 25-31 July 1996 **PA05-062**.
- [45] OPAL Collaboration, R. Akers *et al.*, Phys. Lett. **B353** (1995) 595.
- [46] ALEPH Collaboration, D. Decamp *et al.*, Phys. Lett. **B259** (1991) 377.
- [47] ALEPH Collaboration, ALEPH-Note 93-041 PHYSIC 93-032 (1993);
ALEPH Collaboration, ALEPH-Note 93-042 PHYSIC 93-033 (1993);
ALEPH Collaboration, ALEPH-Note 93-044 PHYSIC 93-035 (1993).
- [48] ALEPH Collaboration, D. Buskulic *et al.*, Z. Phys. **C71** (1996) 357.
- [49] DELPHI Collaboration, P. Abreu *et al.*, Phys. Lett. **B277** (1992) 371.
- [50] DELPHI Collaboration, *Measurement of the Inclusive Charge Flow in Hadronic Z Decays*, DELPHI 96-19 PHYS 594.
- [51] OPAL Collaboration, P. D. Acton *et al.*, Phys. Lett. **B294** (1992) 436.
- [52] OPAL Collaboration, OPAL Physics Note PN195 (1995).
- [53] T. Sjöstrand, Comp. Phys. Comm. **82** (1994) 74.
- [54] G. Marchesini *et al.*, Comp. Phys. Comm. **67** (1992) 465.
- [55] SLD Collaboration, E. Torrence, *Determination of Electroweak Parameters at the SLC*, talk presented at ICHEP96, Warsaw, 25-31 July 1996;
K. Abe *et al.*, Phys. Rev. Lett. **73** (1994) 25;
K. Abe *et al.*, Phys. Rev. Lett. **70** (1993) 2515.
The value of \mathcal{A}_e and $\sin^2\theta_{\text{eff}}^{\text{lept}}$ quoted is an average of the A_{LR} measurement and the left-right and forward-backward left-right asymmetries using leptonic final states.
- [56] CHARM II Collaboration, P. Vilain *et al.*, Phys. Lett. **B335** (1994) 246.
- [57] S. Eidelmann and F. Jegerlehner, Z. Phys. **C67** (1995) 585.
- [58] M. Rijssenbeek, talk presented at ICHEP96, Warsaw, 25-31 July 1996, to appear in the proceedings.
- [59] CDHS Collaboration, H. Abramowicz *et al.*, Phys. Rev. Lett. **57** (1986) 298;
CDHS Collaboration, A. Blondel *et al.*, Z. Phys. **C45** (1990) 361.
- [60] CHARM Collaboration, J.V. Allaby *et al.*, Phys. Lett. **B177** (1986) 446;
CHARM Collaboration, J.V. Allaby *et al.*, Z. Phys. **C36** (1987) 611.

- [61] CCFR Collaboration, K. McFarland, *An improved measurement of $\sin^2 \theta_W$ from neutrino-nucleon deep inelastic scattering*, proceedings of the XV workshop on Weak Interactions and Neutrinos, Talloires France, G. Bonneaud *et al.* eds., Tufts University and L.A.L. Orsay (Sept.1996) vol. II p. 607.
- [62] CDF Collaboration, J. Lys, talk presented at ICHEP96, Warsaw, 25-31 July 1996, to appear in the proceedings.
- [63] DØ Collaboration, S. Protopopescu, talk presented at ICHEP96, Warsaw, 25-31 July 1996, to appear in the proceedings.
- [64] P. Tipton, talk presented at ICHEP96, Warsaw, 25-31 July 1996, to appear in the proceedings.
- [65] UA2 Collaboration, J. Alitti *et al.*, Phys. Lett. **B276** (1992) 354.
- [66] CDF Collaboration, F. Abe *et al.*, Phys. Rev. Lett. **65** (1990) 2243 and Phys. Rev. **D43** (1991) 2070.
- [67] CDF Collaboration, F. Abe *et al.*, Phys. Rev. Lett. **75** (1995) 11 and Phys. Rev. **D52** (1995) 4784.
- [68] DØ Collaboration, S. Abachi *et al.*, *Measurement of the W Boson Mass*, FERMILAB-PUB-96/177-E;
M. Rijssenbeek, talk presented at ICHEP96, Warsaw, 25-31 July 1996, to appear in the proceedings.
- [69] R.M. Barnett, *et al.*, Phys. Rev. **D54** (1996) 1.
- [70] *Reports of the working group on precision calculations for the Z resonance*, eds. D. Bardin, W. Hollik and G. Passarino, CERN Yellow Report 95-03, Geneva, 31 March 1995.
- [71] Electroweak libraries:
ZFITTER: see Reference 40;
BHM (G. Burgers, W. Hollik and M. Martinez): W. Hollik, Fortschr. Phys. **38** (1990) 3, 165;
M. Consoli, W. Hollik and F. Jegerlehner: Proceedings of the Workshop on Z physics at LEP I, CERN Report 89-08 Vol.I,7 and G. Burgers, F. Jegerlehner, B. Kniehl and J. Kühn: the same proceedings, CERN Report 89-08 Vol.I, 55;
TOPAZO: G. Montagna, O. Nicrosini, G. Passarino, F. Piccinnii and R. Pittau, Nucl. Phys. **B401** (1993) 3; Comp. Phys. Comm. **76** (1993) 328.
These computer codes have recently been upgraded by including the results of [70] and references therein.
- [72] T. Hebbeker, M. Martinez, G. Passarino and G. Quast, Phys. Lett. **B331** (1994) 165;
P.A. Raczka and A. Szymacha, Phys. Rev. **D54** (1996) 3073;
D.E. Soper and L.R. Surguladze, Phys. Rev. **D54** (1996) 4566.
- [73] M. L. Swartz, Phys. Rev. **D53** (1996) 5268.
- [74] A.D. Martin and D. Zeppenfeld, Phys. Lett. **B345** (1994) 558.
- [75] H. Burkhardt and B. Pietrzyk, Phys. Lett. **B356** (1995) 398.
- [76] J.P. Martin, *Higgs Particle Searches at LEP*, talk presented at ICHEP96, Warsaw, 25-31 July 1996, to appear in the proceedings.
- [77] R.D. Heuer, *W Mass Determination at LEP II*, talk presented at ICHEP96, Warsaw, 25-31 July 1996, to appear in the proceedings.